Kaunas University of Technology
Faculty of Mechanical Engineering and Design

Fibre Reinforced Polymer Composites Doped with Star Molecules for Automotive Application

Master's Final Degree Project

Rochele Pinto
Project author

Assoc. Prof. Daiva Zeleniakienė
Supervisor

Kaunas, 2021

Kaunas University of Technology
Faculty of Mechanical Engineering and Design

Fibre Reinforced Polymer Composites Doped with Star Molecules for Automotive Application

Master's Final Degree Project
Vehicle Engineering (6211EX021)

Rochele Pinto
Project author

Assoc. Prof. Daiva Zeleniakienė
Supervisor

Assoc. Prof. Sigitas Kilikevičius
Reviewer

Kaunas, 2021

Kaunas University of Technology
Faculty of Mechanical Engineering and Design
Rochele Pinto

Fibre Reinforced Polymer Composites Doped with Star Molecules for Automotive Application

Declaration of Academic Integrity

I confirm the following:

1. I have prepared the final degree project independently and honestly without any violations of the copyrights or other rights of others, following the provisions of the Law on Copyrights and Related Rights of the Republic of Lithuania, the Regulations on the Management and Transfer of Intellectual Property of Kaunas University of Technology (hereinafter – University) and the ethical requirements stipulated by the Code of Academic Ethics of the University;

2. All the data and research results provided in the final degree project are correct and obtained legally; none of the parts of this project are plagiarised from any printed or electronic sources; all the quotations and references provided in the text of the final degree project are indicated in the list of references;

3. I have not paid anyone any monetary funds for the final degree project or the parts thereof unless required by the law;

4. I understand that in the case of any discovery of the fact of dishonesty or violation of any rights of others, the academic penalties will be imposed on me under the procedure applied at the University; I will be expelled from the University and my final degree project can be submitted to the Office of the Ombudsperson for Academic Ethics and Procedures in the examination of a possible violation of academic ethics.

Rochele Pinto

Confirmed electronically

Kaunas University of Technology
Faculty of Mechanical Engineering and Design
Study programme: Vehicle Engineering (6211EX021)

Task of the Master's Final Degree Project

Given to the student:*Rochele Pinto*

1. Title of the Project:

Fibre Reinforced Polymer Composites Doped with Star Polymers for Automotive Application

Automobilių pramonės pluoštu armuoti polimeriniai kompozitai su "žvaigždžių" molekulėmis

2. Aim of the Project:

The aim of the research is to develop a novel hybrid composite material based on epoxy/carbon fibre composites combined with special structured molecules (star-like) with improved mechanical properties for automotive applications.

3. Tasks of the Project:

1. Optimisation and modification of epoxy matrix microstructure with star-like molecules to ensure the improvement of mechanical properties of the matrix material.

2. Experimental investigation of mechanical properties epoxy/carbon fibre composites manufactured using optimised matrix structure.

3. Analysis of low-velocity impact behaviour of novel hybrid composite materials.

4. Comparative analysis of the obtained results with the results of research on relevant materials used in the automotive industry.

4. Structure of the Text Part:

Literature review (several types of additives and fillers and improvement of mechanical properties; experimental investigation; materials for automotive), experimental investigation of star-like additive (mechanical properties), SEM analysis, comparative analysis, results and discussion, references.

5. Consultants of the Project:

Author of the Final Degree Project	Rochele Pinto	2020-02-04
Supervisor of the Final Degree Project	Assoc. Prof. Daiva Zeleniakienė	2020-02-04
Head of Study Programmes	prof. Artūras Keršys	2020-02-04

Pinto Rochele. Fibre Reinforced Polymer Composites Doped with Star Molecules for Automotive Application. Master's Final Degree Project / supervisor Assoc. Prof. Daiva Zeleniakienė; Faculty of Mechanical Engineering and Design, Kaunas University of Technology.

Study field and area (study field group): Transport Engineering (E12), Engineering Science.

Keywords: fibre reinforced polymer composites, star molecules, automotive

Kaunas, 2021. 56 pages

Summary

This project work is an investigation of the effect of novel star-like additives (GTP 463 and GTP 475) on fibre reinforced polymer composites. It consists of a literature survey on various fillers and additives and its effect on the mechanical properties on the carbon fibre reinforced composites (CFRP). The applications of composite materials in automotive components and the trend of the industry to shift from traditional materials such as ferrous metals to composites are discussed.

An experimental investigation is carried out to determine the effects of star-like polymer doped with carbon fibre reinforced polymer composites. This takes place in 2 stages, first an epoxy matrix microstructure with the additives is tested for tensile strength to determine their optimum % to be reinforced with carbon fibres. The second stage involves the testing of the reinforced composites for their tensile, bending and impact capabilities. The tensile tests on the epoxy/GTP 463 showed the improvement in tensile strength of the epoxy matrix with the addition of 3 wt.% of GTP 463 while for GTP 475, an increase in the tensile strength with addition of 1 wt.% of GTP 475 was seen.

Tensile tests on CFRP doped with stars did not show any significant improvement in the tensile strength of the fibre composites due to brittle behaviour. Flexural modulus increased on addition of GTP 475 but no effect with doping of GTP 463. Impact tests on the CFRP specimens doped with 3 wt.% of GTP 463 showed a considerable increase of in the energy absorption capability by 42.84% compared to the reinforcements with pure epoxy matrix. The same results were observed with 1 wt.% of GTP 475, an increase of 29.64% was observed. A brief comparative analysis of the composites investigated with other traditional materials is mentioned.

Pinto Rochele. Automobilių pramonės pluoštu armuoti polimeriniai kompozitai su “žvaigždžių” molekulėmis. Magistro baigiamasis projektas / Assoc. Prof. Daiva Zeleniakienė; Kauno technologijos universitetas, Mechanikos inžinerijos ir dizaino fakultetas.

Studijų kryptis ir sritis (studijų krypčių grupė): Transporto inžinerija (E12), Inžinerijos mokslai.

Reikšminiai žodžiai: pluoštu armuoti polimeriniai kompozitai, žvaigždės tipo molekulės, automobiliai

Kaunas, 2021. 56 p.

Santrauka

Šis baigiamojo projekto darbas apima naujų žvaigždės tipo polimerinių priemaišų GTP 463 ir GTP 475 poveikio pluoštu armuotiems kompozitams tyrimus. Darbe apžvelgiami įvairūs užpildai bei priedai ir jų poveikis anglies pluoštu armuotų kompozitų mechaninėms savybėms. Taip pat darbe aptariamos kompozitinių medžiagų pritaikymo galimybės įvairiuose automobilių komponentuose bei pramonės adaptavimosi tendencijos, pereinant nuo tradicinių medžiagų, tokių kaip metalai, prie kompozitų.

Eksperimentiniai tyrimai buvo atlikti siekiant nustatyti žvaigždės tipo polimerinių priemaišų poveikį, anglies pluoštu armuotiems kompozitams. Darbai buvo suskirstyti į du etapus. Pirmuoju buvo tiriamos epoksidinės matricos su žvaigždės tipo priedais tempiamosios savybės, siekiant gauti optimalų priemaišų kiekį, vėliau naudotiną su anglies pluošto kompozitais. Antrasis etapas apima kompozitų tempimo, lenkimo ir smūgio bandymus. Epoksidinės dervos su 3 masės% GTP 463 tempimo rezultatai parodė, kad atsparumas tempimui padidėjo, tuo tarpu naudojant GTP 475, stiprumo padidėjimas buvo pastebėtas jau prie 1% priemaišų.

Anglies pluoštu armuotų kompozitų su priemaišomis tempimo rezultatai neparodė mechaninių savybių pagerėjimo, galimai dėl mažų deformacijų trūkimo ribos. Tačiau, kompozitų smūgio bandymai su 3% GTP 463 priemaišomis, parodė 42.84% energijos absorbavimo padidėjimą lyginant su įprasta derva impregnuotais kompozitais. Tuo tarpu naudojant 1% GTP 475 priemaišas, gautas 29.64% padidėjimas. Atsižvelgiant į rezultatus, darbe buvo įvertinta kompozitų bei kitų tradicinių medžiagų palyginamoji analizė.

Table of Contents

List of Figures

List of Tables

List of Abbreviations and Terms

Abbreviations:

Assoc. prof. – associate professor.

CNT/CNF – carbon nanotubes/ carbon nanofibres

CFRP/SFRP – carbon fibre reinforced polymer/ short fibre reinforced polymer

wt.% - weight fraction.

CF – carbon fibre.

GHG – greenhouse gases

CVD – chemical vapor deposition

IFSS – interfacial shear strength

Introduction

Application of composites is generally associated with the aerospace industry and high-end luxury and sport cars. However, application of composites in the automotive industry began as early as 1945, when the prototype of a car made with fibre-glass shell was introduced. With increase in research about composites, their applications have proportionally increased. Composites now have their applications in the construction industry and even consumer products. Traditionally, ferrous materials such as cast iron and steel are being used as fail-safe due to their low cost of production and strength, however, with the shift of focus to sustainability, reducing emissions, achieving fuel-efficiency, and improving ride safety and quality while maintaining the standard of strength and performance, has become critical. Composites have been sought after to fulfil these ever-growing demands in the transport industry. While composites have higher material costs, they compensate by providing overall weight reduction, improving efficiency of fuel consumption, and therefore reducing operating costs. Added advantages of using composites are corrosion-resistance, greater thermal conductivity, and better impact performance. With the ongoing research on recyclability of composites, the issue of waste produced by their one-time use and throw is addressed.

Reinforcements like carbon, glass fibres, etc. have lower scope of improvement compared to the enormous possibilities of improving the polymer matrix associated with composites. Properties such as damage tolerance and impact behaviour where fibres fall short, the properties of the matrix come into perspective. Matrix of a composite helps uniformly disperse the load to each fibre providing better load handling capabilities. In the automotive industry, 3 criteria for material response that need to be fulfilled by the polymer-matrix composites (PMC) are durability, energy absorption and ride quality. Additional criteria for the application of PMC are unambiguous evidence of improvement of properties, consistent manufacturing, and effect on economically associated aspects [1]. The incorporation of specific additives and fillers, helps tweak the properties of the matrix materials to suit the requirements of their use. 2-D and 3-D nanoparticles such as MXenes, carbon nanotubes (CNTs) etc. or star-shaped additives in small quantities have known to increase the strength of composites.

This work of research is a detailed investigation of such an additive synthesized by SYNPO, an industrial company in Czech Republic that works with high-profile automotive companies and provides composite solutions that cater to specific requirements by their clients. With the company's collaboration, its mechanical properties, capabilities of improving the composite and overall properties are investigated to determine its correct application and usage in the transport industry. A comparative analysis with other relevant materials being used in the transport industry will provide an insight and serve as a justification of its suitability as a contender to traditional materials.

Aim of the Project: The aim of the research is to develop a novel hybrid composite material based on epoxy/carbon fibre composites combined with special structured molecules (star-like) with improved mechanical properties for automotive applications.

Tasks of the Project:

1. Optimisation and modification of epoxy matrix microstructure with star-like molecules to ensure the improvement of mechanical properties of the matrix material.

2. Experimental investigation of mechanical properties epoxy/carbon fibre composites manufactured using optimised matrix structure.

3. Analysis of low-velocity impact behaviour of novel hybrid composite materials.

4. Comparative analysis of the obtained results with the results of research on relevant materials used in the automotive industry.

1. Literature Survey

1.1. Application of Composites in the Automotive Industry

1.1.1. Automotive Components and Composites

Traditionally, automotive components are being made of ferrous metals such as iron, steel, etc. but with the shift focusing to sustainability, the need for materials that help reduce greenhouse gas (GHG) emissions and make fuel consumption efficient, are on the search. Composites provide similar or even greater advantages to these conventional metals by reducing the overall weight of vehicles. Vehicular weight and engine power majorly influences a vehicle's fuel consumption. Therefore, implementing lightweight materials could significantly decrease the costs related to fuel consumption and CO_2 emissions [2].

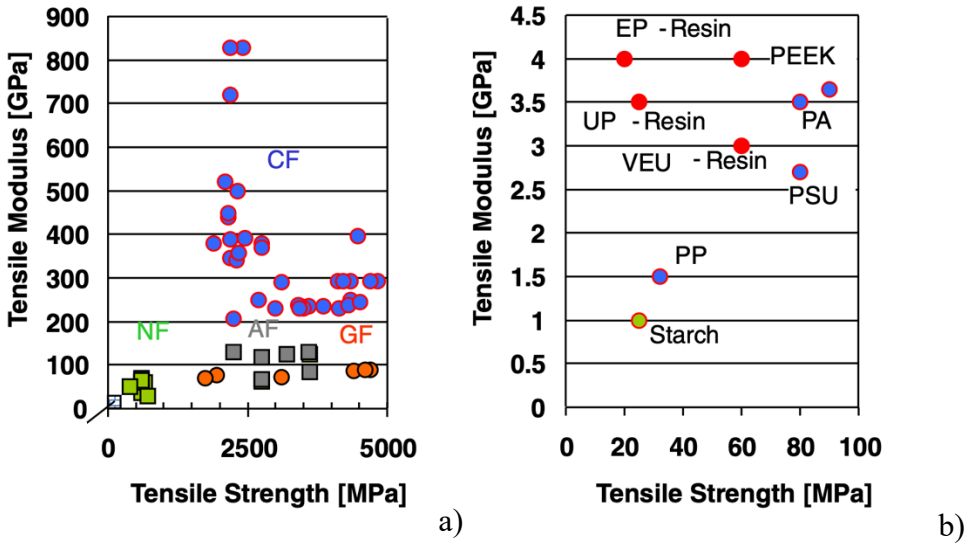

Fig. 1. Tensile strengths of reinforcements and matrices a) modulus of various fibre reinforcements b) modulus of various polymeric matrices [3]

With the development of electric vehicles, intricate and detailed designs are being incorporated to increase performance. The demand to create such complex geometries cannot be kept up with conventional monolithic metals. Metals unlike composites cannot have their properties tweaked to suit the requirement. Composites comprise of 2 components, matrices, and reinforcements, which can individually be tweaked to produce materials that satisfy specific applications. There are 4 main components that comprise of a vehicles weight which are, power train, its structure, exterior and interior. Table 1 shows current and emerging trends of materials being used in these automotive components.

Table 1. Material trends in automotive industry [4]

	Material Trends in the Automotive Industry	
Automotive Components	**Current**	**Emerging**
Power Train (Engine, Transmission, Suspension)	Steel, Iron and Aluminium	High-Strength Steel (HSS)/Advanced High-Strength Steel (AHSS)
Structural (Chassis)	Steel, HSS/AHSS	HSS/AHSS, Aluminium, Composites
Exterior (Doors, Bumper, Hood, Trunk)	Steel, Aluminium, Plastics, Composites	Steel, HSS, Aluminium, Plastics, Composites

Interior (Dashboard, Floor, Inner door panel, Seats, Steering)	Steel, Plastics, Composites	Plastics, Composites

We see that the future of the materials used in the automotive industry inclines towards composites. Each of the reinforcements bring different properties and therefore can be applied in specific components according to their strengths as shown in Table 2.

Table 2. Applications of composites in automotive components [4]

Type of Composites	**Applications (Automotive Components)**
Carbon Fibre Composites (high specific strength, electrically conductive, low coefficient of thermal expansion)	Chassis, Roof, Tailgate, Hood, Floor Panel, Trunk, Fender, Bumper
Glass Fibre Composites (high tensile strength, heat resistance, corrosion resistance)	Air-Intake Manifold, Bumper Beam, Engineer Cover, Air Duct
Natural Fibre Composites (recyclability, biodegradable, low energy consumption)	Inner Door Panels, Seat Backs, Load Floor

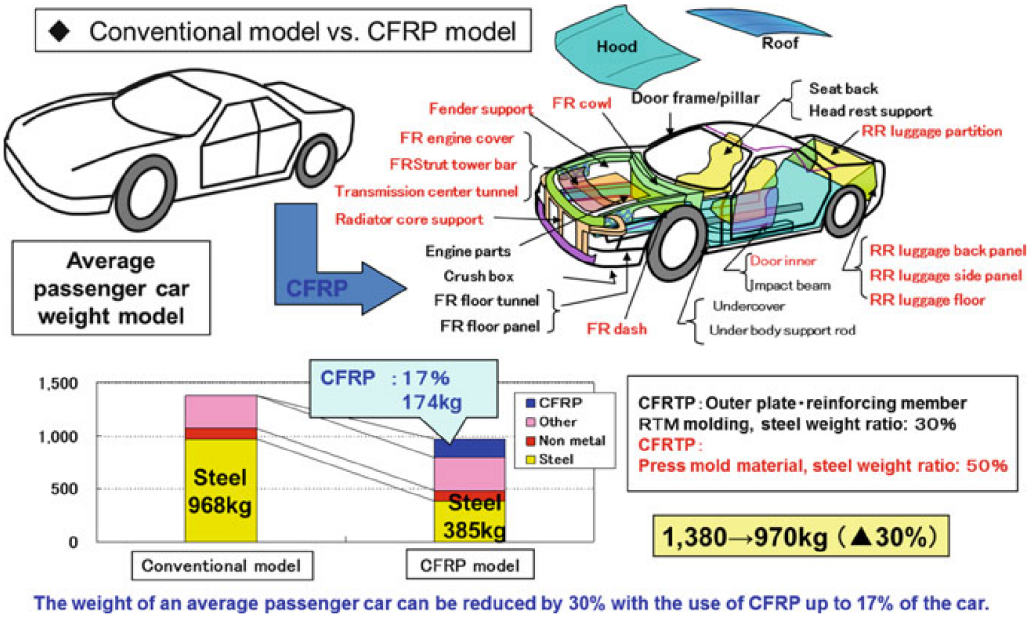

Fig. 2. Weight reduction by implementing CFRP model [5]

In the Figure 2, we see that by implementing a CFRP model instead of a conventional model reduces the overall weight from 1,380 kg to 970 kg, a reduction of 30% by the inclusion of just 17% of CFRP manufactured components [5]. However, the foremost obstacle for industries to switch from metals to composites is the cost factor. Compared to metals, composites are costly to purchase, and large-scale mass production is difficult to implement. Figure 3 shows how composites compensate inflated purchasing cost with lowering costs related to fuel consumption and reduction in the emission of CO_2.

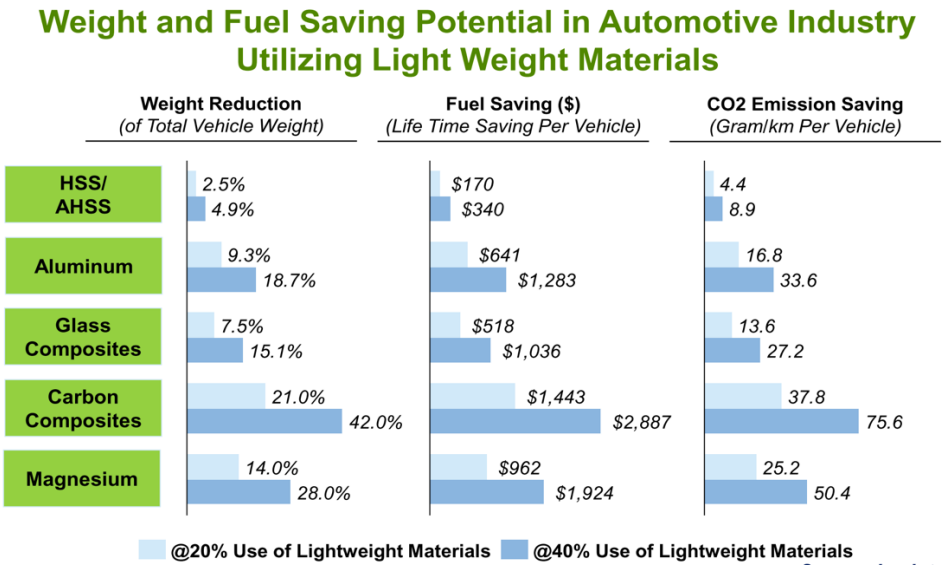

Fig. 3. Potential of composites in automotive industry [4]

A crucial factor in the application of any material to a vehicle is its crashworthiness. Its capability to absorb energy to avoid any injury to seated passengers is a critical aspect. Legislation states that an impact velocity of 15.5 m/s should provide no injury to the passengers seated inside. Carbon fibres have low damage tolerance however the improvement of the matrix can increase the crash absorption ability of the composite. Composite materials have brittle characteristics, while metals have ductile. Traditional materials on impact undergo buckling while composites undergo various forms of failure, such as, fibre rupture, matrix cracking, delamination, de-bonding etc. The crash response in composites depends on numerous factors, such as fibre orientation, geometry, properties of matrix, etc. These factors can be designed according to the requirement of its application.

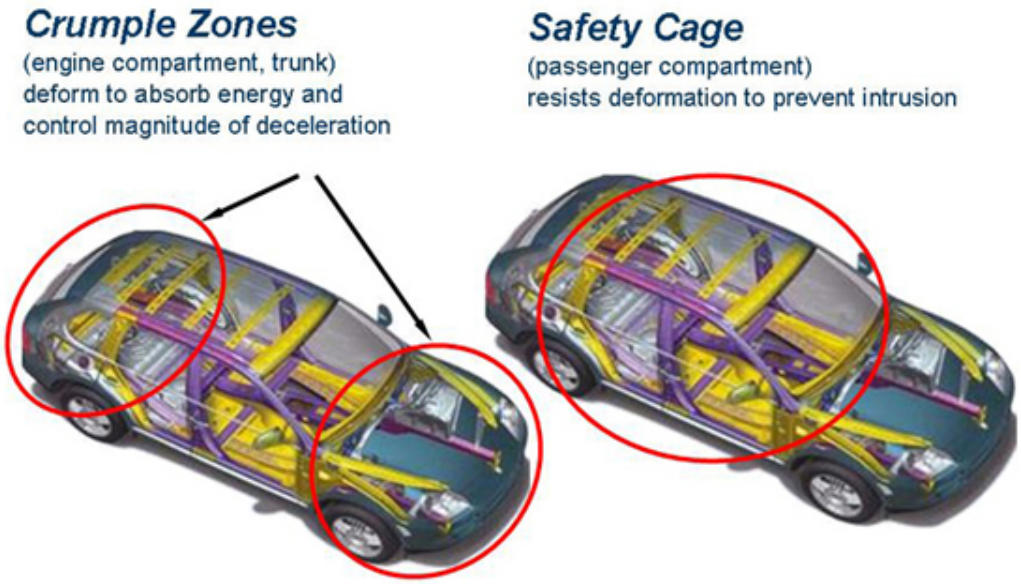

Fig. 4. Crumple zones in a crash collision

In Figure 4, we see the concept of crumple zones. Vehicles are built to crumple to provide safety in the event of an unfortunate collision. The front and rear components of the vehicle should be designed with materials that absorb the maximum percentage of the impact force before the effect reaches the

safety cage (passengers). The dissipation of crash energy through the vehicle components is illustrated in Figure 5.

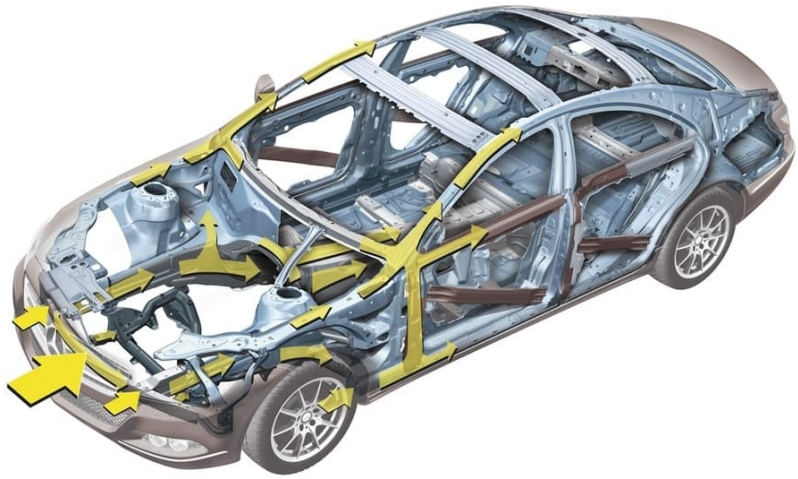

Fig. 5. Crash force dissipation [6]

In Figure 6, the specific energy absorption (SEA) of various materials that are used in automotive components is displayed by the means of a bar graph.

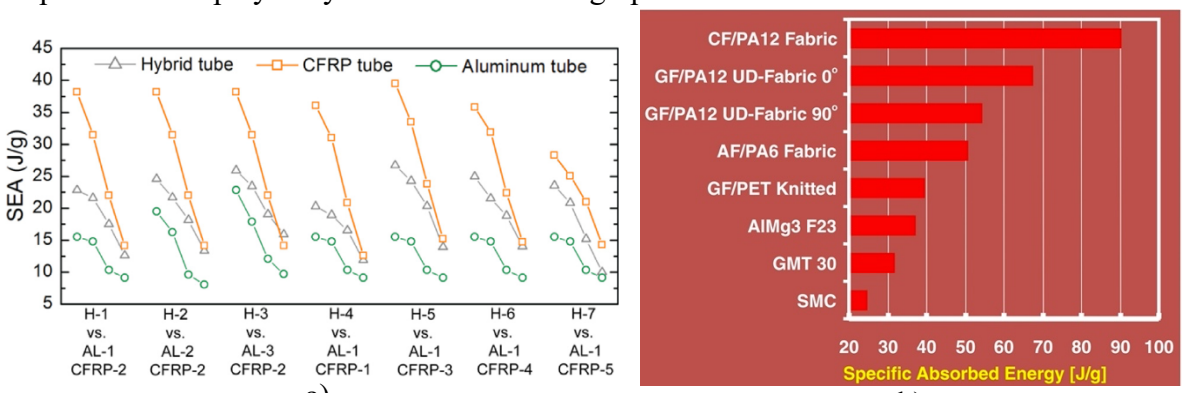

a) b)

Fig. 6. Specific Energy Absorption (SEA) capabilities between a) metals vs composites [7] b) different composites [3]

Figure 6a, is a graph plotted between the SEA of an aluminium tube, CFRP tube and a hybrid tube made of CFRP and aluminium. In both a and b, carbon fibre polymer composites show the best SEA rates.

1.1.2. Matrixes, Fibres, Lamina Stacking Sequence used in Automotive Components

Achieving light-weight cars is among the significant strategies of sustainable growth, which are of considerable value for both reduction of exhaust emissions and protection of the environment, can be achieved by using alternative, lightweight materials. Composite materials are suitable for this reason due to their excellent tensile capabilities and great stability. The application of composite materials in the automotive industry, therefore, has a long history of helping to produce environmentally friendly and energy-efficient vehicles while at the same time achieving weight loss. Composite sandwich systems are composed of strong thin panels on the outside and light, thick foam type elements in the core. Such structures can withstand loads as traditional structures, even though lighter

in weight. There is distribution of the load onto the panels and the core material. The central substance has a certain influence on the bending and torsional stiffness. There are several types of sandwich construction component components, including rubber, honeycomb frameworks, and corrugated sheets [8].

Torsional stiffness is a crucial consideration that evaluates the performance of the composite driveshaft. A modern mechanical theoretical approach of torsional stiffness for the composite drive shaft with balancing laminate is extracted from traditional lamination theory and mechanical research [9].

Composite sections are composed of carbon fibres pre-preg with an epoxy matrix. The layers are put in the mould until they are enclosed in the bag and positioned under vacuum. The sealed component is then put in an autoclave where it is subjected to the prescribed temperature and pressure process needed to cure the matrix content. The passenger cell often contains sandwich frameworks where layers of composite material are mounted on either side of a plastic or aluminium foam sheet to provide an incredibly durable and lightweight component. The engine carriage at the rear of the car is fastened to the passenger cell to form the main load-bearing structure. External body panels are bolted to the structure of the chassis and are non-structural components. The manufacturing process is labour-intensive and not appropriate for high-volume production. The possible approach for the manufacture of composite vehicle components includes the usage of liquid moulding methods in combination with the strengthening of non-crimp (NCF) cloth [10].

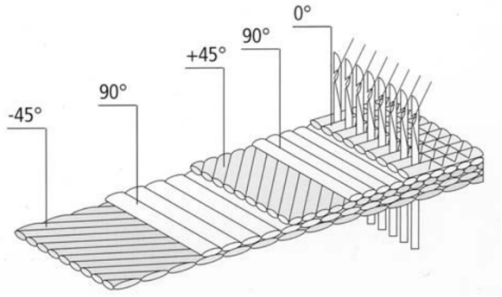

Fig. 7. Manufacturing of multi-axial non-crimp fabric reinforcement [10]

The cost related to manufacture and moulding pre-pregs other than carbon fibre could be dramatically reduced [11]. In closed-loop recycling, where the recycled carbon fibre will be used to re-engineer vehicle components, problems associated with loss in strength while removing the resin [12]. Short-fibre reinforced polymer (SFRP) composites are incredibly desirable due to easy manufacture, economicability, and excellent mechanical properties [13].

1.2. Diversity of 2D and 3D Nanoparticles for Properties Improvement

An experiment was conducted to test and analyse the effect of growing carbon nanotubes in situ on carbon fibre cloth. The process of chemical vapor deposition (CVD) was performed at 900°C and pressure of 500 MPa to grow the carbon nanotubes (CNTs) on the surface of the fibres. By guiding the time for electroplating and deposition, different percentages, and irregular aligned deposition of CNTs by weight were observed on the surface of individual fibres.

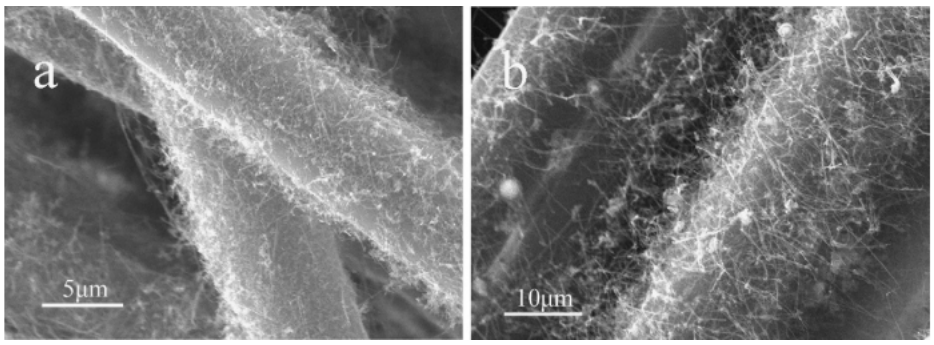

Fig. 8. In-situ growth of CNTs on carbon fibre surface [14]

Three-point bending testing for flexural strength was applied and an average of the values was presented. Conclusively, an increase in flexural strength and modulus in the vertical direction was close to 30% and 70% respectively and in the parallel direction, 60% and 50% respectively [14]. In the process of chemical grafting, the CNTs were grafted through a chemical reaction on carbon fibres in the form of fabric. The CNT grafted through the CVD saw an increase in tensile strength by 11% and the fibres grafted by chemical method showed an increase of 20% in the same[15] [16].

Carbon fibre reinforced with polytetrafluoroethylene (PTFE) as a filler proves to be resistant to wear. PTFE is tough, self-lubricating, and is less soluble which proves resistance to abrasive wear and tear. In recent studies, the inclusion of graphene filled composites is investigated due to its fantastic thermal, mechanical, and electrical properties. Therefore, a study by on the effective thermal deposition of graphene oxide (GO) without compromising the tensile strength of the fibres was formed to observe an enhancement of mechanical properties of carbon fibre reinforced PTFE. The GO deposition increased the surface roughness of carbon fibre causing better bonding between the resin and matrix. With the homogenous deposition of GO, creates better wettability between the carbon fibre (CF) and the resin. With a 5-minute deposition, the shear strength was observed to increase from 49.5 to 71.91 MPa. The graphene oxide on the surface of CF functioned as a protecting layer to help alleviate stress concentration and preventing the cracked edges to create deviation of the crack path. The tensile strength was observed to be improved by 5.39% [17].

Researchers investigated that electrical grade CNT (XD-CNT) which consists of double and single-walled nanotubes were cheaper and had higher-yielding strength. Amino-functionalized XD-grade CNTs (involving a mixture of single, double, and multi-walled CNTs) improved interfacial adhesion and enhanced the thermal and mechanical properties of the matrix. The bulk stiffness and strength were investigated where an increase in flexural strength and modulus by 14% and 27% was observed by addition of 0.3 wt.%. Additionally, the functionalization with amine was proved to improve properties. A 19% improvement in tensile strength was seen in the 0.3 wt.% loading. It was seen that uniform loading of XD-CNTs was crucial for good interfacial adhesion [18].

MXene is a new 2-D transition metal carbide and or nitrides with a unique structure that has piqued the interest of researchers due to its different thermal, mechanical, and electrical properties when included in the resin. A research highlights how carbon fibre reinforced epoxy composites by MXene nanosheets coating led to an increase in flexural, tensile, shear, and impact strength of the composites. The process of creating the carbon fibre and MXene composite is shown in the figure below:

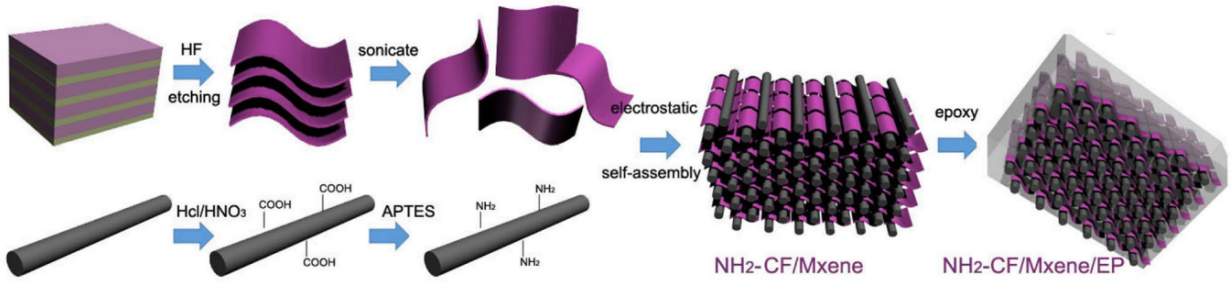

Fig. 9. Illustration of the process of creating NH_2-CF/MXenes/EP composites [19]

The NH_2-CF/MXenes/EP composites increase the tensile, flexural, shear, and impact strength by 40.8%, 45.9%, 38.5%, and 74.4% respectively. The MXene nanosheets act as a supplementary reinforcement for interfacial adhesion, reducing interlaminar stress and increasing the toughness of the carbon fibre [19].

We know that carbon fibres have excellent longitudinal properties i.e., their strength and toughness are concentrated longitudinally but poor transversal strength. A study concentrated on improving the transverse properties of carbon fibre by magnetically aligning multi-wall carbon nanotubes to the fibres. Five sample groups within which four more samples were created, the 1st one with only resin, the 2nd with resin + 1.5 wt.% MWCNTs, 3rd with carbon fibre reinforced polymers laminates without CNTs, the 4th with CFRP + 1.5 wt.% CNTs with no magnets and the 5th with CFRP + 1.5 wt.% CNTs with nanoparticles with the application of a magnetic field during the process of curing. The results were significant with an increase in flexural modulus by 46% compared to the non-aligned CNTs. It also led to an increase in the load-bearing ability by 33% [20].

J. Leng *et al.* suggested using a low velocity to track failure of CFRPs as they are hard to track internally. In this model, the impact of the velocity of not more than 10 m/s is recorded to allow the CFRP to counter and the propagation of the stress wave need not be studied. The failure of the material would be due to delamination, cracks in the matrix, and breakage of the fibres. The addition of graphite fluoride (GrF) could suppress the cracks which are critical in the matrix and therefore increasing its impact properties. GrF was added to the mixture of epoxy and hardener with various weights from 0 wt.% to 4 wt.%. The composite laminates were fabricated by a vacuum-assisted resin transfer modelling process (VARTM). The application of pressure of 0.26 MPa was done to ensure a constant fibre volume fraction and laminate of uniform thickness of 2.5 mm. A cure cycle was performed, the dwelling of 4 hours at 50°C and 6 hours at 70°C. Series of tests were held such as drop-weight impact, ultrasonic C-scan evaluation, etc. The 1 wt.% absorbed the least amount of energy which suggested the least damage. The variation in GrF content causes a fluctuation crack pinning, crack deflection, etc. When the GrF content is low, these effects toughen the matrix whereas an increase in the same creates an overwhelming effect on the toughness. The 1 wt.% also showed the highest compressive strength, with any quantity less or more showed deprecating behaviour [21].

An investigation by records the improvement in mechanical properties of carbon fibres in the form of fabric using carbon nanofibers (CNF). Vapor-grown carbon nanofibers (CNFs) attract considerable attention to nano-scale polymer reinforcement due to their high tensile strength, modulus, and relatively low cost. Previous findings showed that adding lesser quanitites of CNF (<3 wt.%) to the matrix could improve the thermal and mechanicalcapabilities. An improvement in flexural modulus of around 22.3% was noticed with a mixture of 2 wt.% CNF [22].

1.3. Star Molecules as an Additive to Improve the Mechanical Properties of Carbon Fibre reinforced Polymer Composites

1.3.1. Polyhedral Oligomeric Silsesquioxane (POSS)

Silsesquioxane's cage-like structure is a crossbreed of silicon and oxygen with likenesses to both silica and silicone. At the point when blended in with for all intents and purposes like any normal polymer, they attach to the natural particles and each other, framing huge chains that weave through the polymer. The outcome is a nanostructured natural inorganic cross breed polymer. The POSS chains act like nanoscale fortifying filaments, delivering remarkable gains in heat resistance [23].

Carbon fibres were grafted with octa-glycidyl dimethyl silyl POSS were analysed for the improvement of mechanical properties between the matrix and the fibres.

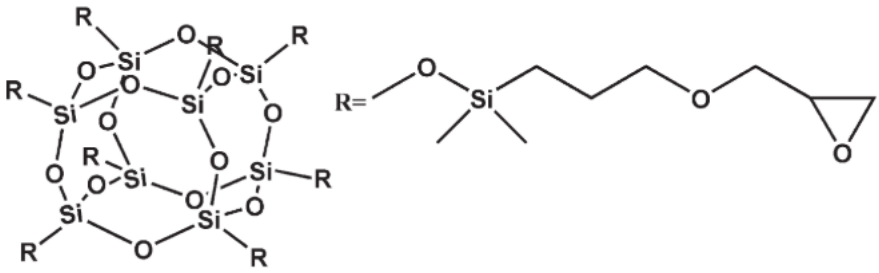

Fig. 10. Structure of octa-glycidyl dimethyl silyl POSS [24]

In the testing of mechanical properties, it could be seen that the POSS grafting substantially increased the IFSS of the composites by 31.5%. The increase could be attributed to good bonding between the fibres and the matrix. After alteration, the POSS epoxy groups improved interfacial adhesion between the fibres and matrix [24]. The use of POSS as a novel coupling agent between the carbon fibre matrix and epoxy, for the functionalization of traditional carbon fibres, resulting in improvement in the polarity and roughness of the fibre surface and increase the composite's IFSS by increasing wettability and bonding [25].

Conventional POSS is deemed to be expensive, L. Ma *et. al* self-synthesized an octa-(γ-chloropropyl) POSS since amine-functionalized CF proved to as a better matrix for surface adhesion with the resin. The process of grafting hyper-branched POSS on the surface of the carbon fibres is illustrated in the following diagram:

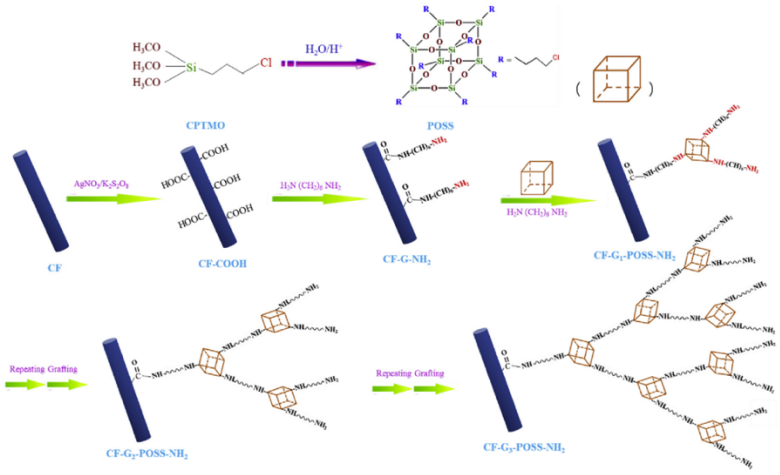

Fig. 11. Functionalization of hyperbranched POSS onto carbon fibres [26]

It was seen that the interfacial efficiency of composites was largely dependent on the generation of functionalization. In fact, CF-G_3-POSS-NH_2/EP composites showed the maximum growth, i.e., 87.9% in interfacial shear strength and 83.7% in interlaminar shear strength relative to untreated carbon fibre and epoxy composites. In turn, the storage modulus, and the glass transition temperature of had also improved significantly [26].

The effects of coating silsesquioxane on carbon fibres reinforced with polyarylacetylene (PAA). Carbon fibres were coated with a variety of materials, including[3-(methacryloxy) propyl] tri-methoxyl silane (MPMS), [3-(methacryloxy)propyl] silsesquioxane (MPMS-SSO) and (methacryloxy)propyl polyhedral oligomeric silsesquioxane (methacryl-POSS) by hydrolytic condensation. The ILSS of untreated carbon fibre and PAA composites was 30.2 MPa, indicating weak bonding between fibre and resin. ILSS of matrix and resin composites treated with MPMS coating decreased by 8%, and composites coated with MPMS-SSO and methacrylic-POSS coatings improved by 42% and 34%. The nanocage arrangement of methacrylic-POSS helps uniformally distribute the load and transfer it from the PAA resin to the CF [27]. F. Zhao *et. al* used carbon nanotubes (CNTs) as nanofillers in the composite by chemical vapor deposition on the fibres of carbon. The process of formation of carbon fibre-octa-glycidyl di-methyl silyl POSS-CNTs is shown as below:

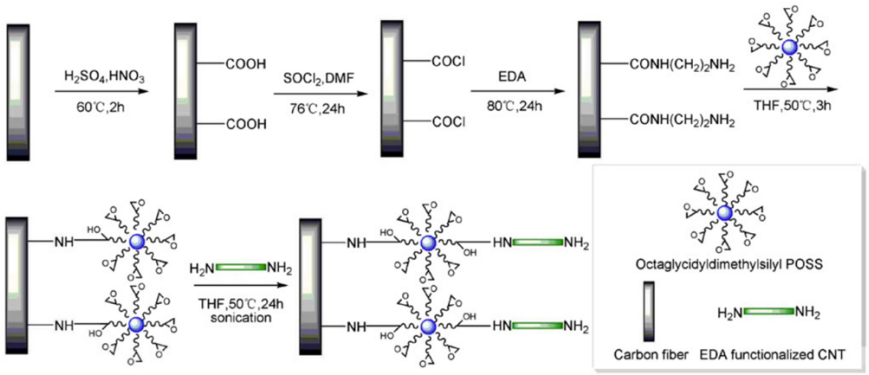

Fig. 12. Schematic formation of CF-POSS-CNTs [28]

Mechanical properties of the composites were evaluated, and the tests indicated increased ILSS and impact strength. The surface roughness of the fibers was enhanced for POSS-grafted fibres. The functionalization overall increases the bonding by employing epoxy groups on the POSS [28].

1.4. Experimental Investigation of Mechanical Properties of Carbon Fibre Reinforced Polymer Composites

A study adopts micro-laser line thermography (micro-LLT) to detect micro-sized defects in CFRP [29]. Laser line thermography (LLT) is performed to find cracks in surfaces. D. Li *et. al* converted a laser spot to a laser line point using a beam expander and a cylindrical lens [30]. Tracking of certain forms of defects, however, has been badly reported. X-ray computed tomography (CT) has become familiar as a usable research method for NDT of materials and components, it is also attracting increasing attention recently related to the latest appearance of several large enterprises. A research was conducted to evaluate the capacities and weaknesses of micro-CT for FRP composites, in which various test samples with a range of failure types, shapes and sizes were examined to measure the impact of device resolution on the ability to evaluate the internal structure of defects, like delamination, matrix fracture, and on the surface certain micro porosities [31]. Optical micrographs and microstructural investigation were conducted to approximate the void quantity and to describe the void structure, position, and scale of carbon fibre/polyetheretherketone (PEEK) plate [32].

Infrared thermography is a technique of successful and controllable detection thermal pulsed, cycled, and ultrasonic excitation. After collection, analysis, and processing of infrared image sequences, prompt finding, and quantitative analysis of the defect within the objects can be performed [33]. A study also implemented vibrothermography (VT), the energy is generated internally in VT [34]. VT, also known as ultrasonic thermography, uses mechanical waves to specifically activate inner voids and not increase the temperature of the surface.

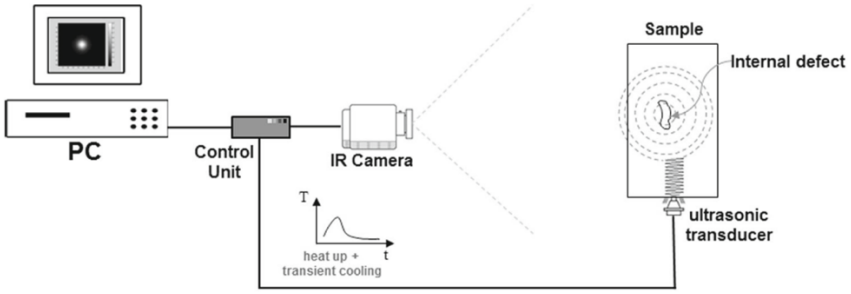

Fig. 13. Vibrothermography [34]

Damage is most commonly measured by non-destructive techniques (NDT) such as usage of ultrasonic and eddy currents, performed on damaged specimens instead of during damage infliction. Observation after damage infliction provides tracking of situation, while observation during damage infliction gives a clearer perception of the origin, process, and extent of damage. Furthermore, examination post-damage infliction enables the identification of irreversible results, though observation of damage infliction identifies reversible and permanent results. A non-destructive method used while damage is inflicted is acoustic emission, however this method provides no information on how reversible the damage is and detects only major effects produced [35] [36]. Electrical resistance measurement was implemented to detect strain and defects in CFRP composites [37]. Damage caused by breakage results in an increase in the electrical resistivity in the fibre's direction increases, whereas damage caused by delamination increases resistivity in the thickness' direction. Acoustic emission detection only detects strain associated with deformation. Fibre damage is more drastic than matrix damage, as fibres are much stronger than the matrix. [38]. Electrical resistance measurement can also be implemented to study the damage caused by any kind of impact,

like the four-probe method to sense the damage caused by impact in a carbon fibre polymer-matrix composite [39].

2. Methodology for the Investigation of Star Molecules

This chapter provides an insight into the details about the polymer additive in focus. It highlights in brief the chemical composition of the additive, process for sample preparation and the necessary mechanical testing carried out to investigate the properties and strength of the material for automotive application.

A schematic representation of the methodology approach is depicted in Figure 14. The process of investigation takes places in 2 stages, first the preparation of the epoxy resin specimens and the mechanical testing of the matrix to determine optimum % of star molecules. Second, the reinforcement of the matrix with carbon fibres and its mechanical testing.

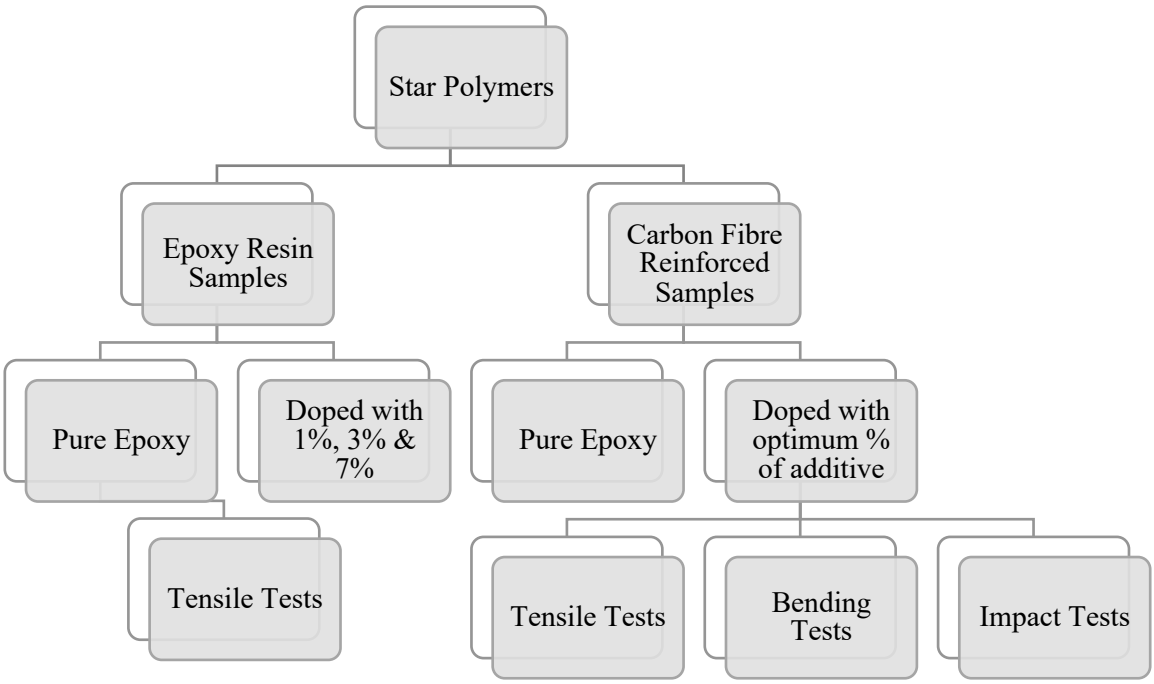

Fig. 14. Methodology

2.1. Materials

A composite comprises essentially of 2 components, the matrix and reinforcement. The primary matrix was formed by a mixture CHS Epoxy 582™, a bisphenol-A epoxy resin of low molecular weight that contains reactive diluent (1,4-butanediol diglycidyl ether) to reduce viscosity and Telalit 0420™ (isophorone diamine) hardener which is a cycloaliphatic amine (supplied by Spolchemie, Czech Republic). The additives, GTP 463 and 475 are star-like polymers (also known as stars or star molecules) used to increase the strength of the matrix (synthesized by SYNPO, Czech Republic). Bidirectional twill woven (2/2) carbon fibre fabric was used as reinforcement. Properties of the fabric are mentioned in Table 3.

Table 3. CF fabric properties [40]

Properties of Carbon Fiber Fabric	
Tensile Strength (MPa)	3500
Tensile Modulus (GPa)	240
Density (g/cm^3)	1.79

Linear Density (tex)	200

2.1.1. Star Molecules

GTP 463 & 475 are solid, dry, butyl methacrylate (BMA) polymers that appear star-like at the molecular level and are stored in 50% tetrahydrofuran (THF) as a solution. The solution contains stars (consisting of core and arms) and free unbuilt arms, both of BMA. GTP 463 is a homopolymer of n-BMA while GTP 475 is a copolymer, with units of glycidyl methacrylate (GMA) at the end of the arms. The molecular weight of the polymer is determined by Gel Permeation Chromatography (GPC), a type of Size Exclusion Chromatography (SEC). In this method, 2 phases, a porous solid packing material usually a type of gel (polystyrene) is placed a column (the stationary phase) and the polymer (analyte) and a solvent, also called the eluent (THF) (mobile phase) is made to flow through this stationary phase [41].

The theory behind the process of separation, as illustrated in Figure 15, is that varied sizes of molecules of the analyte elute at separate times as the smaller molecules would enter the pores, while the larger molecules may not fit in these pores of the packing material. Therefore, larger molecules would leave the column first followed by molecules of decreasing size, determining the concentrations of these molecules [41].

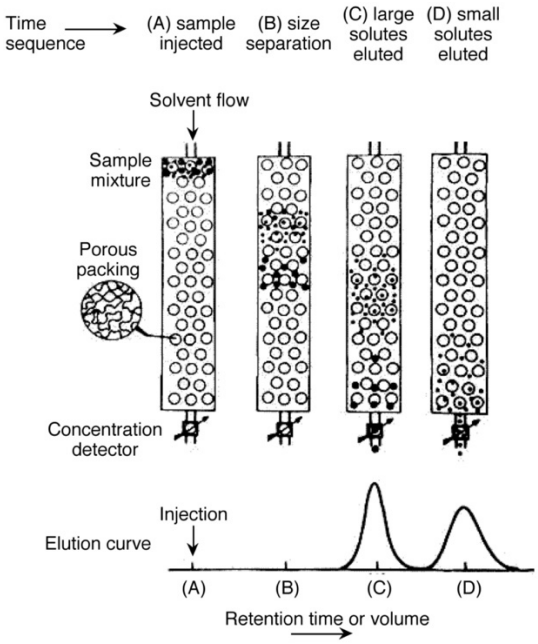

Fig. 15. Process of separation [42]

A refractive index detector is placed after the column that detects the analyte in the solvent due to the differences in the indices of solvent and analyte and thereby detects the concentration of the molecules displayed by a chromatogram. The below chromatograms (Fig. 16 & 17) display the results of the refractive index detector with the detector response (in mV) against the elution volume (in millilitres). A volume of 100 uL (microlitre) of each were injected separately. The results of the GPC are displayed below the chromatograms (Table 4).

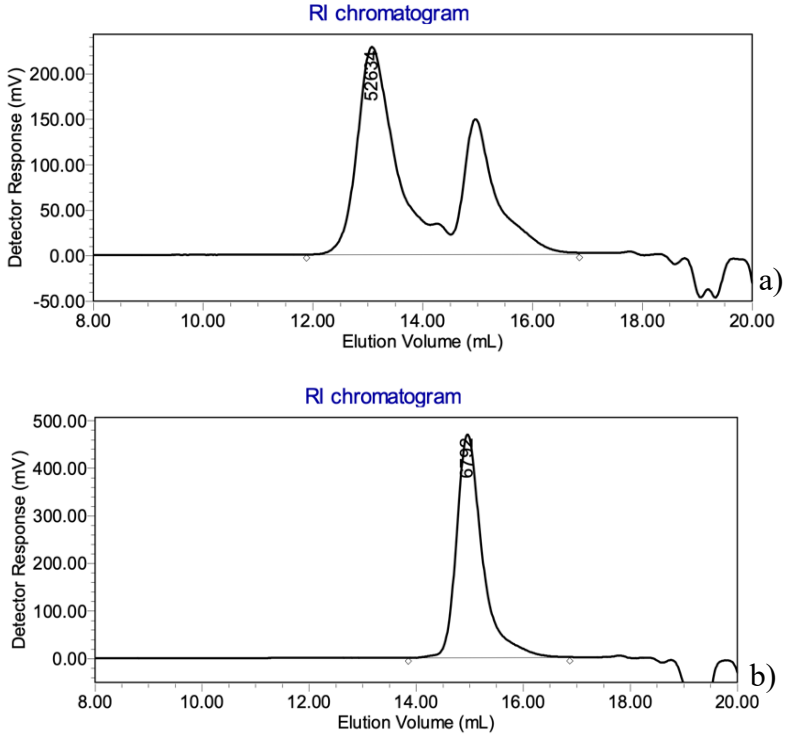

Fig. 16. GPC chromatogram of GTP 463 a) Star b) Free Arms

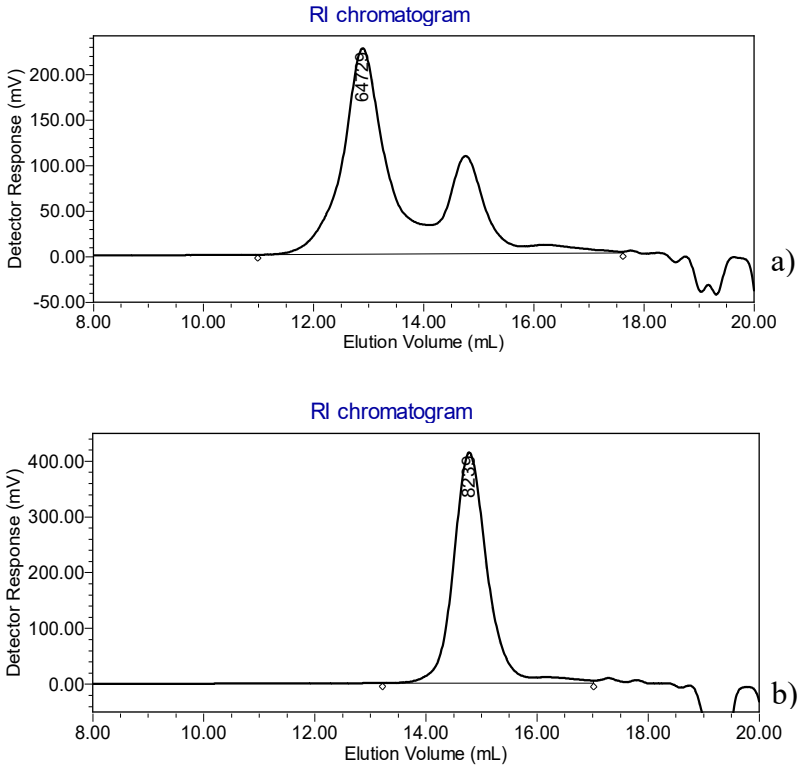

Fig. 17. GPC chromatogram of GTP 475 a) Star b) Free Arms

Table 4. GPC results

	Properties of GTP 463 & 475						
		Mn	**Mw**	**MP**	**Mz**	**Mz+1**	**Polydispersity**

GTP 463	Star	10915	32494	52634	52625	63227	2.98
	Free Arms	5625	6378	6792	6934	7426	1.13
GTP 475	Star	12152	50657	64729	89752	131386	4.17
	Free Arms	6510	8155	8239	9357	10737	1.25

Mn – number average molecular weight. It is the total weight of the polymer divided the number of molecules; Mw – weight average molecular weight. It is the mass of the individual chains that makes up the overall weight of the polymer; Mz, Mz+1 – weight average molecular weight with number of chains 2 and 3 respectively; MP – molecular weight of the highest peak. Polydispersity – (Mw/Mn) is an index for the distribution of the polymer chain within the polymer. All weights expressed in g/mol or Da.

2.2. Specimen Preparation

To investigate the tensile strength and effect of the additive in the epoxy, 3 different wt.% were chosen – 1 %, 3 % and & 7 % to incorporate in the epoxy. Dog-bone shaped moulds were prepared according to ISO 527-2-5A (Testing Tensile Properties of Plastics). The matrix comprised of epoxy resin and hardener that were mixed in the ratio 100:25 respectively Increase in the percentage of additive increased the viscosity of the mixture at room temperature, increasing the presence of micro-bubbles and a cloudy appearance. These bubbles were unable to escape during the degassing in the vacuum pump due to its viscosity. The additive was soluble in the hardener, however on pouring of the epoxy, the same issue reoccurred.

The mixture of the epoxy and additive was then heated above the boiling point of THF (66°C) to evaporate the solvent. The viscosity of the mixture reduced, and the mixture started clearing up with the bubbles rising to the surface. Once the mixture had negligent bubbles, the temperature was lowered below 50°C, to ensure that the curing process did not occur prematurely on addition of the hardener. Since the temperature of the epoxy and additive mixture was higher than room temperature, the hardener mixed in easily, however, the working time of the epoxy reduced significantly. The epoxy mixture was then degassed in the vacuum chamber for 5-10 minutes after which it was poured into the moulds. After placing the moulds at room temperature overnight, they were cured in the oven for 2 h at 60°C, 1 h at 80°C and 1 h at 120°C.

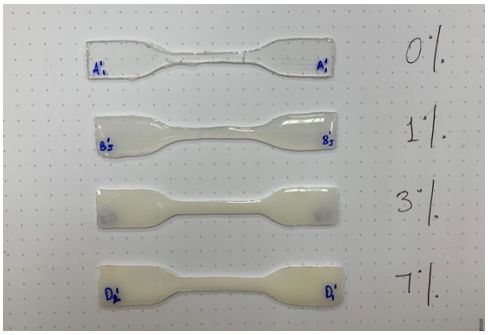

Fig. 18. Epoxy tensile specimens with different additive wt. %

The carbon fibre specimens of 300 mm x 300 mm were created with wet hand layup technique. 5 layers of prepreg carbon fibre fabric were cut out to achieve a thickness of 1 mm. A layer of polyvinyl alcohol (PVA), a releasing agent was applied on which a layer of the epoxy resin was poured. A layer

of prepreg carbon fibre fabric was laid and completely wetted out. The process was repeated until all plies of the fabric were laid out. A porous peel ply followed by a breather plate was placed to wick the excess resin. The entire set-up was then vacuum bagged and left overnight. The samples were then cured in the oven for 2 h at 60°C, 1 h at 80°C and 1 h at 120°C. The samples were then machined and smaller samples of desired dimensions for further testing were cut out. The optimum wt. % from the tensile tests performed on the GTP/epoxy specimens, was then used to reinforce with carbon fibre.

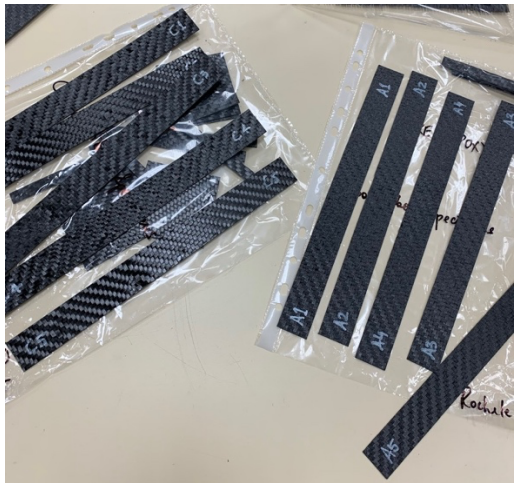

Fig. 19. CFRP specimens

2.3. Experimental Testing

2.3.1. Tensile Tests

Tensile tests specimens for epoxy resin were prepared according to ISO 527-2-5A standard [43]. The overall length of the specimen measured 80±1 mm with gauge length of 25 mm and thickness of 2 mm. The testing was performed on H10 KT universal column testing machine (Tinius Olsen, UK) with maximum applicable force of 10 kN and 'Horizon' software. The crosshead movement rate was 2 mm/min. 5 samples were used to reduce error in the results. 4 sets of samples were prepared for each GTP 463 and 475. Pure epoxy, and epoxy doped with 1, 3 and 7 wt.%. Load – extension measurements were obtained

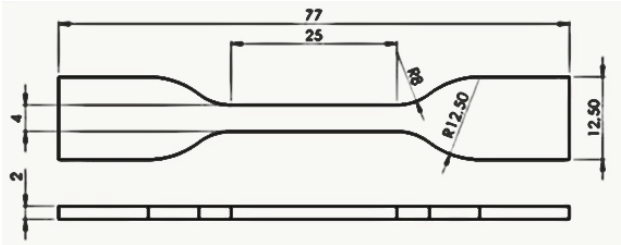

Fig. 20. ISO-527-2-5A specimen dimensions [47]

For carbon fibre specimens, ASTM D3039 standard (Standard Test Method for Tensile Properties of Polymer Matrix Composite Materials) was referred. The dimensions of the specimens are provided in Table 5. Abrasive material was used as end tabs to avoid slippage in the grips. The testing was performed. The testing was performed on H50 KT universal column testing machine (Tinius Olsen, UK) with maximum applicable force of 50 kN and 'Horizon' software. The crosshead movement rate

was 2 mm/min. 5 samples were used to reduce error in the results. The experimental set-up is shown in Figure 21.

Table 5. CFRP tensile test dimensions

Specimen Dimensions (mm)	
Overall Length	250±50
Gauge Length	150
Length of End Tabs	50±25
Width	25
Thickness	1±0.1

Fig. 21. Experimental set-up for CFRP tensile testing

From the load-extension measurements, stress, strain, and Young's modulus was calculated by equations (1), (2) and (3).

$$\sigma_{tensile} = \frac{F}{A} \tag{1}$$

$$\varepsilon = \frac{\Delta L}{L} \tag{2}$$

$$E_t = \frac{\sigma_2 - \sigma_1}{\varepsilon_2 - \varepsilon_1} \tag{3}$$

If: σ – stress (MPa); F – tensile force (N); A – cross-sectional area (mm^2); ε – strain; ΔL – extension produced in the specimen (mm); L – total length of specimen (mm); E_t – tensile modulus (MPa); σ_2/σ_1 – stresses at strains ε_2 and ε_1 respectively (MPa).

2.3.2. Bending Tests

3-point bending tests were performed on CFRP specimens prepared according to ASTM 7264 standard (Standard Test Method for Flexural Properties of Polymer Matrix Composite Materials).

The testing was performed on H10 KT universal column testing machine (Tinius Olsen, UK) with maximum applicable force of 10 kN and 'Horizon' software. 3-point bending grips were used. The crosshead movement rate was 2 mm/min. 6 samples were used to reduce error in the results. The support span and width ratio can be taken from anywhere between 16:1 to 60:1. Specimen length should not exceed 20 % of the support span. Dimensions of the specimens are provided in Table 6. Tests were performed on the specimens until failure. Load – extension measurements were obtained.

Table 6. CFRP bending test specimens

Specimen Dimension (mm)	
Overall Length	130
Support Span Length	70
Width	13
Thickness	1±0.1

From the force – extension measurements, bending stress was calculated by the Equation 4.

$$\sigma_{bending} = \frac{My}{I} = \frac{3Fl}{2bd^2} \quad (4)$$

The flexural modulus for long beam strength is given by the formula,

$$E_f = \frac{l^3 m}{4bd^3} \quad (5)$$

If: σ – bending stress (MPa); F – bending force applied (N); l – support span (mm); m – slope of load-deflection curve (N/mm) at deflections at 2 and 2.5 mm; b/d - breadth and thickness of specimen (mm).

2.3.3. Impact Tests

Low-velocity instrumented puncture tests were performed on 5 carbon fibre specimens according to ISO 6603-2 (Puncture Impact Behaviour of Rigid Plastics). This standard requires specimens to be of circular or square shape. The dimensions of the specimens were 60 mm × 60 mm and 1±0.1 mm thick. High-speed drop tower (Coesfeld GmbH & Co. KG, Germany) was used to perform the experiment. The mass of the impactor was 5.185 kg and was dropped from a height of 0.4 m. The tip of the impactor is blunt and hemispherical with diameter 20 mm. The velocity of impact calculated by Equation 5 is 2.80 m/s. The experiments were conducted at room temperature. Force – time plots were obtained. The depth of the deflection, force and energy at 3 different points were measured:

- When the impactor strikes and damages the specimen.
- At maximum force exerted.
- At puncture of the specimen.

From the force-time graph, acceleration was calculated. Double integration of the acceleration provided the displacement at every time interval [44]. The contact force and displacement in turn gives the energy absorbed by the specimen. According to standard ISO 6603-2, the force-time graph depicts different values of forces such as, force at damage, maximum force, and force at puncture of specimen [45]. At these points of force, the equipment also measures the energies and the deflection caused by the forces on the specimens. Similar graphs of force and energies at the deflection points are plotted below (Fig. 5).

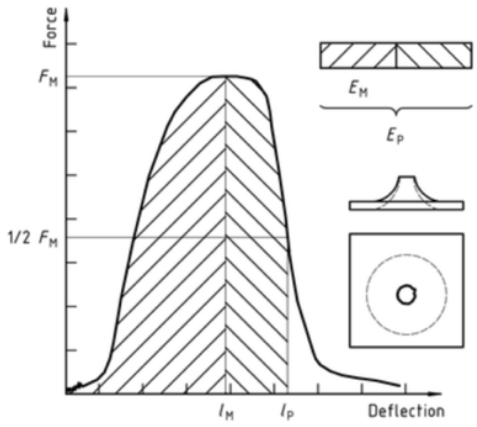

Fig. 22. Force-deformation curves (according to ISO 6603-2) [49]

In drop weight impact testing, potential energy of the impactor is converted to kinetic energy at impact. We calculate the energy by first calculating the velocity at impact by Equation 6:

$$v = \sqrt{2gh} \tag{6}$$

Therefore, kinetic energy at impact is given by equation

$$K.E = \frac{1}{2}mv^2 \tag{7}$$

3. Results & Discussion

This chapter discusses the results and analysis of the tests performed in the above section.

3.1. GTP 463

3.1.1. Tensile Test

Epoxy/GTP 463

Tensile tests performed on samples of the epoxy-additive specimens were used to analyse the optimum percentage of stars that made an impact on the strength of the epoxy matrix. The results from the machine measured tensile force (N) and the extension (mm). Stress (MPa) and strain (%) were calculated from equations (1) and (2) and plotted (Fig. 23). Young's modulus was calculated from the chord slope of the curves (equation 3)[46]. The results of the tensile tests are presented in Table 7.

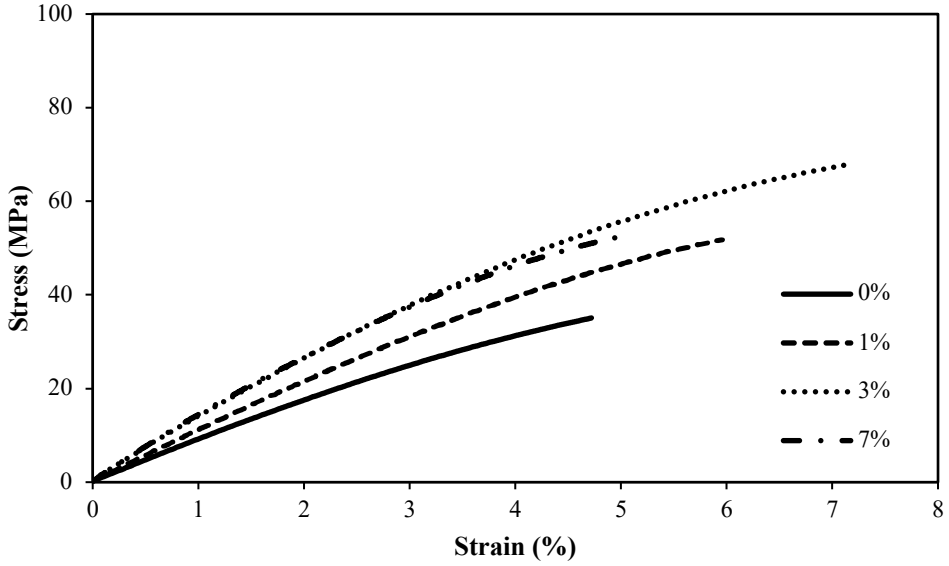

Fig. 23. Stress-strain curves for different wt.% of GTP 463

Table 7. Tensile test results

Material	**Maximum Force at Break (N)**	**Maximum Stress (MPa)**	**Maximum Strain (%)**	**Young's Modulus (GPa)** (At ε_2=1.25% and ε_1=1%)
Pure Epoxy	289.60	35.09	4.72	0.87
1 wt. % GTP 463	415.00	51.79	5.96	1.06
3 wt. % GTP 463	487.50	68.07	7.20	1.28
7 wt. % GTP 463	370.80	55.55	5.88	1.33

We see in Table 7 that the addition of 3 wt. %, shows increase in maximum stress and Young's modulus by 93.99 % and 41.47 % from pure epoxy. For 7 wt. %, we see an increase in Young's modulus by 52.63 % even though the stresses in the specimens are lower. This depicts the brittleness of the specimens. Therefore, the optimum % of addition of GTP 463 could be 3 wt.% or between 3 and 7 wt.%. In Figure 24. we see that with increase in the wt.% of the additive, the gain in modulus

is maintained while a decrease in tensile strength is observed. This is owing to the brittle nature and incorporation of micro bubbles that effectively reduce load handling capabilities.

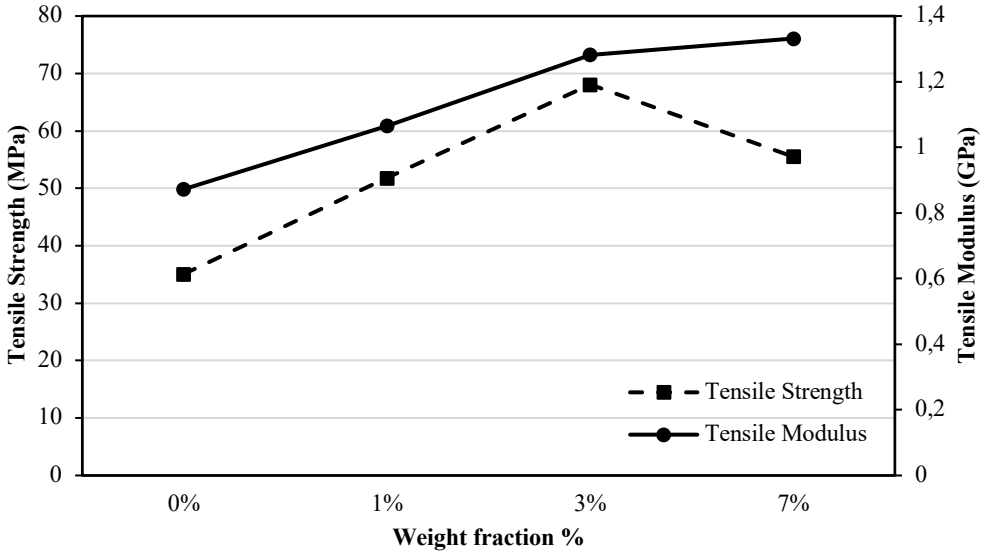

Fig. 24. Trend of tensile strength and tensile modulus with increase in wt.%

CFRP/GTP 463

Tensile tests on CFRP with pure epoxy and doped with 3 wt.% were tested for tensile strength. The complete results are provided in Appendix 1. Tensile strength, strain and tensile modulus were calculated using equations (1), (2) and (3). Tensile stress against the strain is plotted in Figure 25.

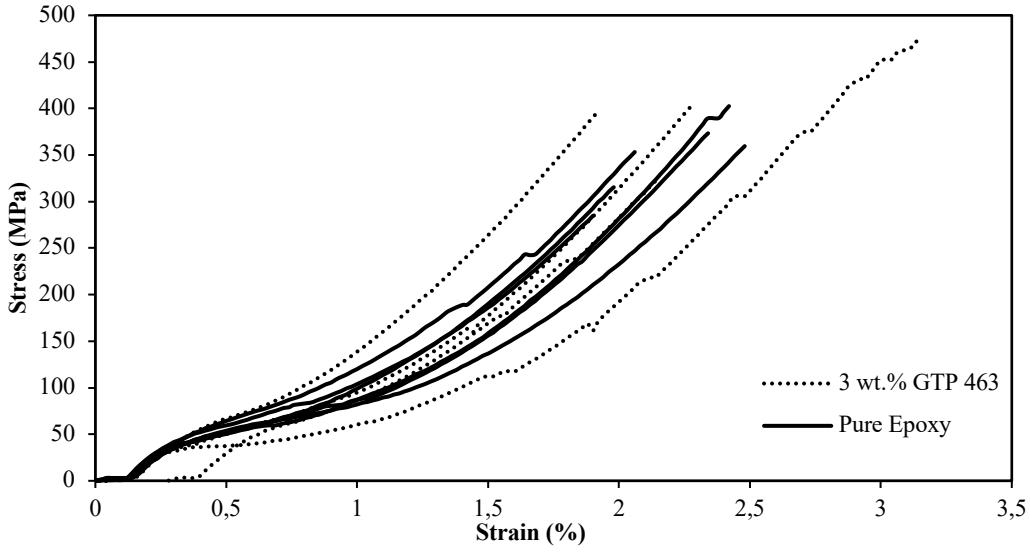

Fig. 25. Stress - Strain Curves for CFRP specimens

Table 8. Tensile test results for CFRP specimens

Material	**Maximum Force at Break (kN)**	**Maximum Stress (MPa)**	**Maximum Strain (%)**	**Tensile Modulus (GPa) (At ε_2=0.02% and ε_1=0.25%)**

Pure Epoxy	7116.20	284.65	1.90	13.59
3 wt.% GTP 463	9926.70	397.07	1.92	13.97

We see that the tensile modulus of the CFRP specimens is low due to their bidirectionality. Unidirectional fibres along the axis of the load applied perform better under tensile tests. The properties of the composite are also dependent on the individual properties of the fibre and matrix. We see that the specimens exhibit brittle behaviour due to similar tensile modulus showing that the properties of the matrix are governing the results of the test as carbon fibres exhibit high tensile strength.

3.1.2. Bending Tests

3-point bending tests were performed on CFRP specimens doped with 3 wt.% of GTP 463. The bending stresses and flexural modulus were calculated from equations (4) and (5). The force versus deflection produced in the specimen is plotted below in Figure 26. The results of the tests are provided in Table 9 and Appendix 2.

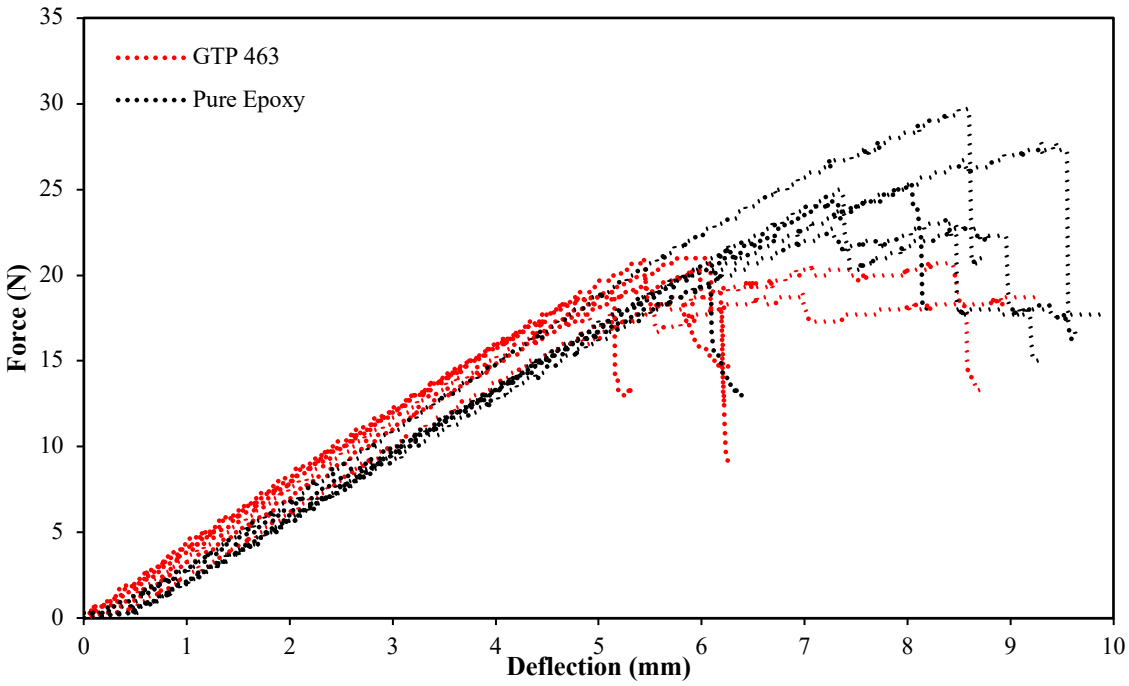

Fig. 26. Force vs deflection plot

Table 9. Bending test results

Material	**Maximum Bending Force (N)**	**Maximum Stress (MPa)**	**Deflection at Maximum Stress (mm)**	**Flexural Modulus (GPa)**
Pure Epoxy	25.30	204.34	8.04	22.62
GTP 463	20.10	162.34	6.15	26.30

It is observed that the doping of CFRP specimens with GTP 463 improves the bending properties of the material slightly. Improvement is seen in flexural modulus by 16.27%. The flexural modulus of a specimen is dependent on numerous factors such as the thickness of specimen, the support span length used for the test. The specimens doped with GTP 463 are stiffer than that of pure epoxy.

3.1.3. Impact Tests

Fibre reinforced epoxy specimens doped with 3 wt.% of GTP 463 were investigated under impact. For this test, the contact force (kN) and contact time (ms) were measured at every instant. The punctures specimens are shown in Figure 27. The complete results of the test performed is given in Appendix 3. The force – time measurement from the impact test is plotted in Figure 28.

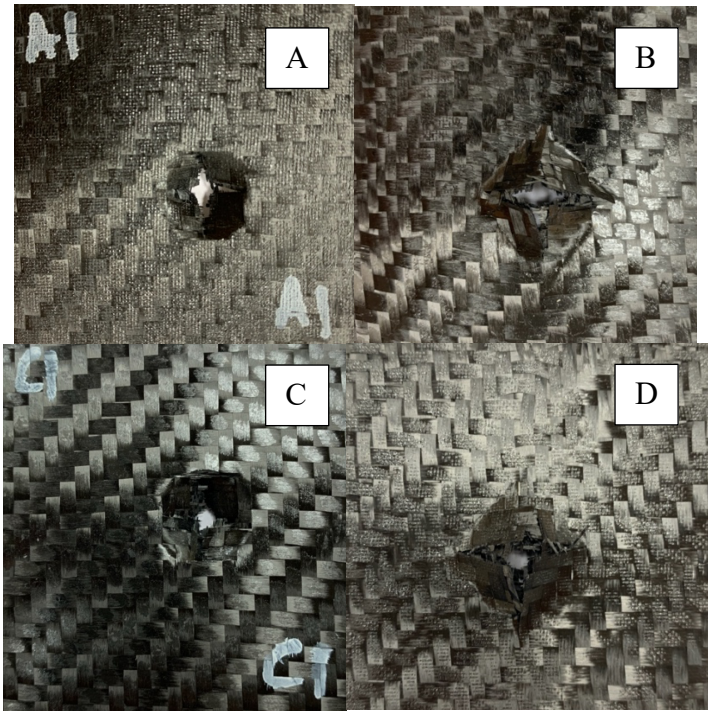

Fig. 27. Punctured impact test specimens (with top and bottom views) *A, B: pure epoxy*; *C, D - 3 wt.% GTP 463*.

The failure in impact specimens occurs in 2 modes namely, catastrophic failure and progressive failure [47]. Catastrophic failure occurs due to unstable intra and inter-laminar structure failure which is visible by a sudden sharp spike in peak load and then a lower failure load while progressive failure is controlled and progresses through the specimen according to the crushing speed. It is usually caused by creating a defect at specific location to observe the crack growth. Energy absorbed in a progressive failure is higher than that in a catastrophic failure.

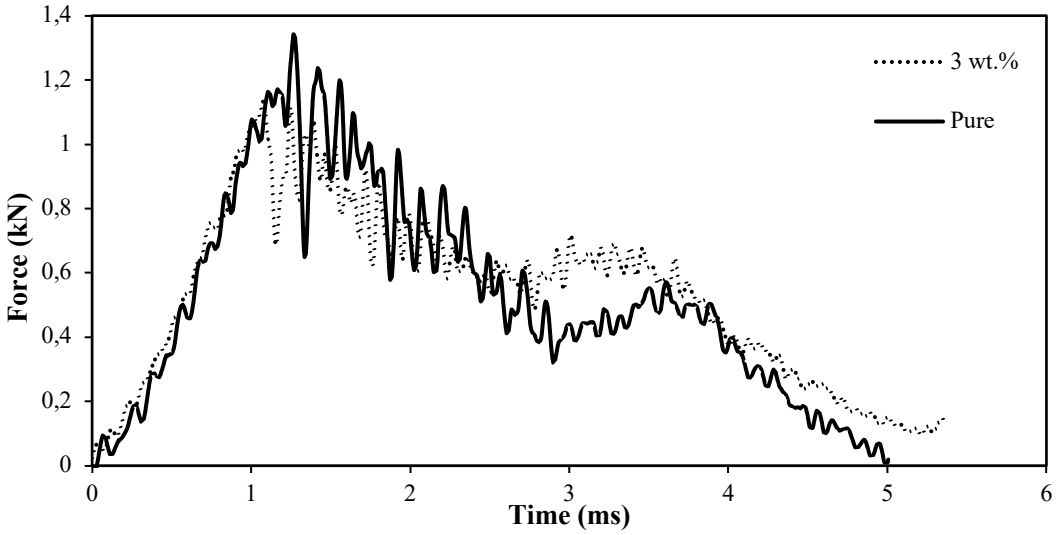

Fig. 28. Force-time graph for carbon fibre reinforced epoxy specimens

In Figure 29, the subscript '*D*' denotes the first instance the specimen is damaged. The puncture '*P*' of the specimen occurs at half the maximum force exerted on the specimen [45]. These plots show that the force required to puncture the specimens of 3 wt. % is 1.13 kN, compared to 1.35 kN for pure epoxy. The deflection at puncture for pure epoxy is 2.54 mm while for the additive specimens is 4.63 mm showing that the ability of the GTP 463 specimens to compress and absorb the energy better causing higher deformation since both have a proportional relationship. The energies plotted above are at the point of damage, maximum force and point of puncture. The absorbed energy against the displacement is plotted below (Fig. 6).

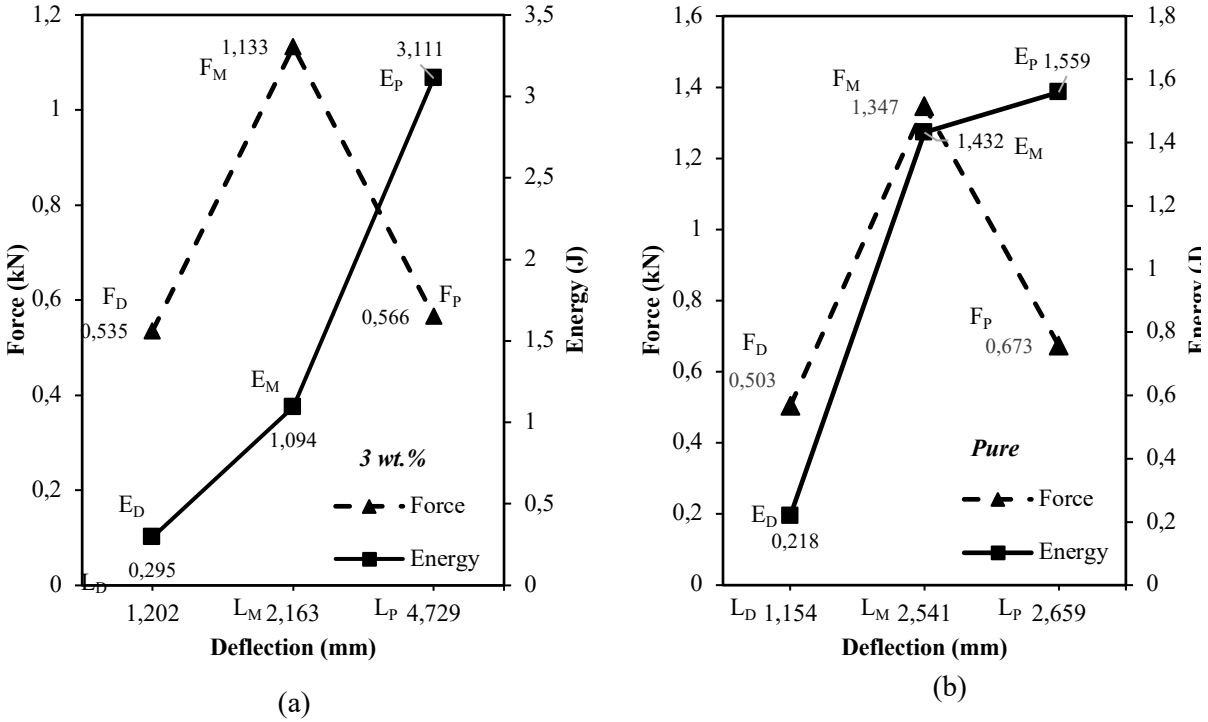

Fig. 29. Force-deflection-energy plots (a) – GTP 463 (b) – Pure Epoxy. *F – force; L – deflection; E – energy; M – maximum; P – puncture; D – damage.*

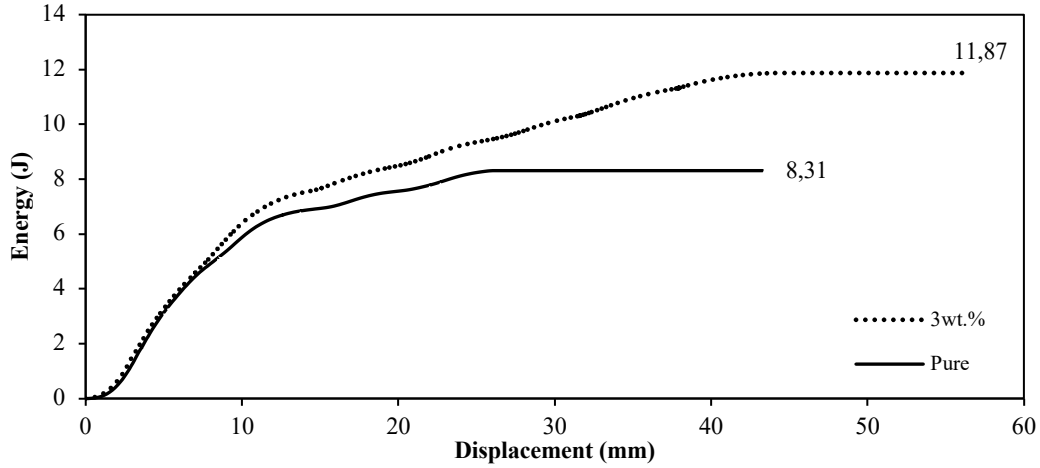

Fig. 30. Absorbed energy vs time plot

Figure 30 shows that the specimens with additives absorbed a greater amount of energy compared to the pure epoxy specimens. The former absorbed a total of 11.87 J of energy while the latter absorbed only 8.31 J of energy which is an increase by 42.84 %. The ability of impact energy absorption is mainly dependent on the matrix as fibres have poor impact resistance. Therefore, the energy at impact is mainly absorbed by the matrix

3.2. GTP 475

3.2.1. Tensile Tests

Epoxy/GTP 475

Tensile tests performed on samples of the epoxy-additive specimens were used to analyse the optimum percentage of stars that made an impact on the strength of the epoxy matrix. The results from the machine measured tensile force (N) and the extension (mm). In Figure 31 we see the stress strain curves of the different wt.% calculated from equations (1) and (2).

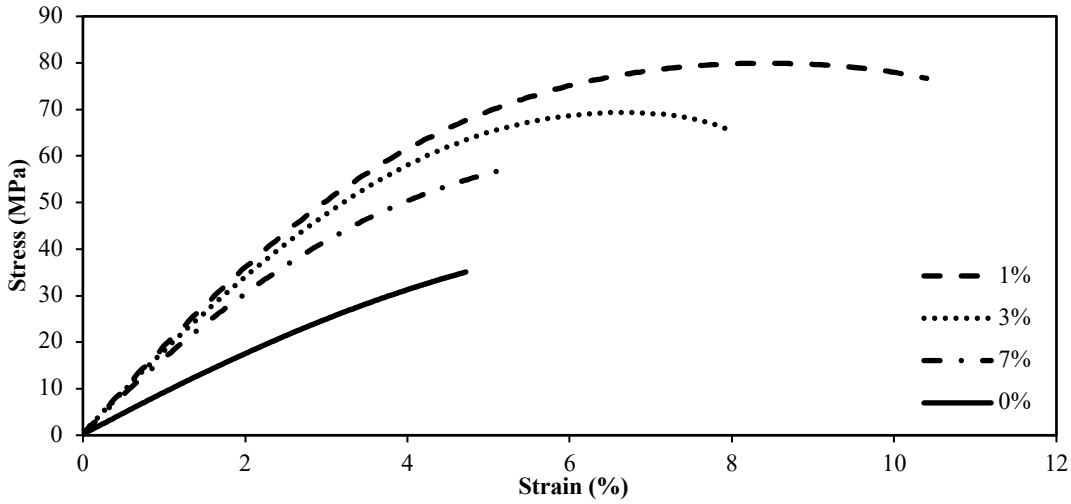

Fig. 31. Stress- strain curves for different wt.% of GTP 475

We see that the addition of 1 wt.% shows the most improvement in the tensile strength. The maximum tensile stress for 1 wt.% of GTP 475 is double the stress for pure epoxy. There is a gain in modulus with addition of 3 wt.% however an observed decrease in tensile strength and modulus with addition of 7 wt.% as seen in Figure 32.

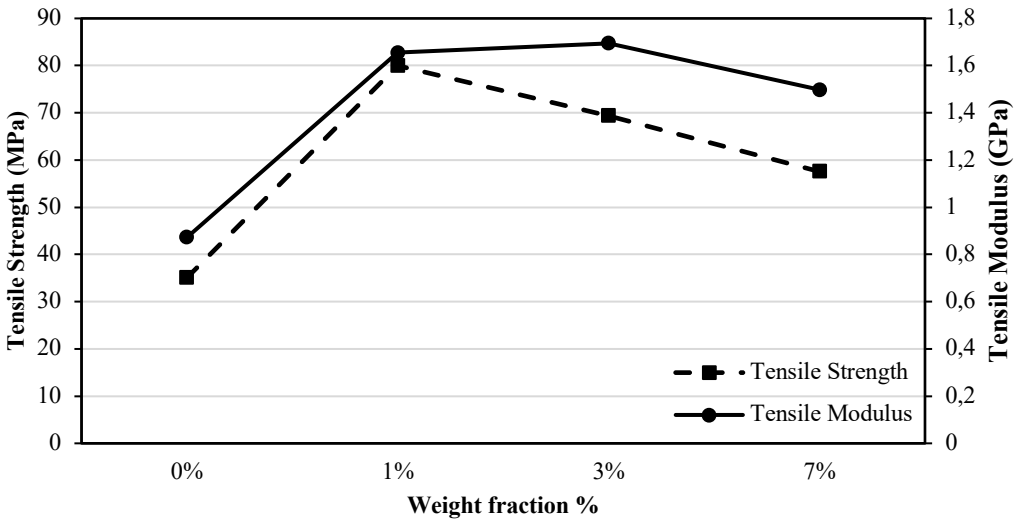

Fig. 32. Trend of tensile strength and tensile modulus with increase in wt.%

Table 10. Tensile test results

Material	**Maximum Force at Break (N)**	**Maximum Stress (MPa)**	**Maximum Strain (%)**	**Young's Modulus (GPa)** (At ε_2=0.02% and ε_1=0.25%)
Pure Epoxy	289.60	35.09	4.72	0.87
1 wt. % GTP 475	434.5	79.99	2.12	1.65
3 wt. % GTP 475	386.4	69.35	1.71	1.69
7 wt. % GTP 475	329.6	57.58	1.33	1.49

CFRP/GTP 463

Tensile tests on CFRP with pure epoxy and doped with 3 wt.% were tested for tensile strength. The complete results are provided in Appendix 1. Tensile strength, strain and tensile modulus were calculated using equations (1), (2) and (3). Tensile stress against the strain is plotted in Figure 33.

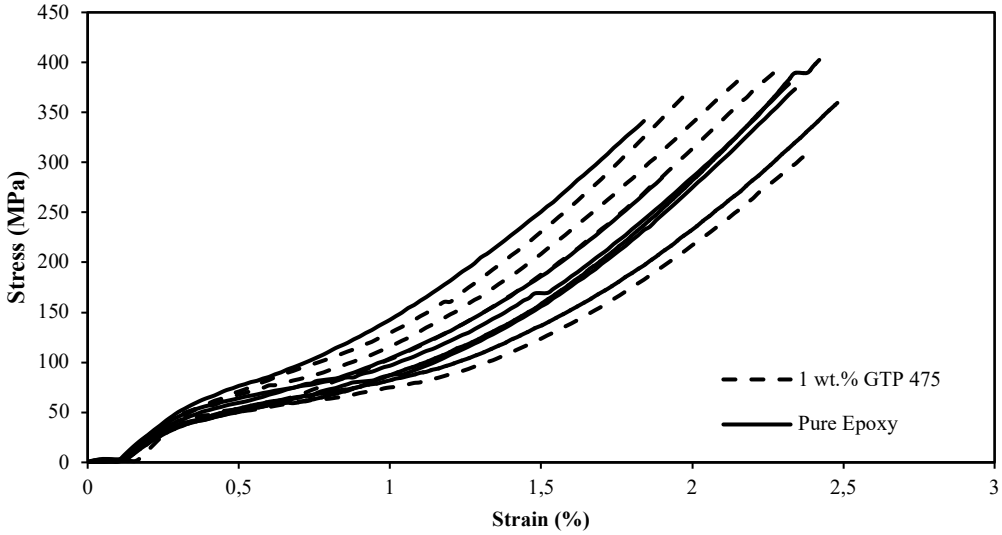

Fig. 33 Stress - strain curves for CFRP specimens

From Table 11 we see that there is a slight improvement in the tensile strength and modulus of the additive specimens. The strain produced in the specimen is lower as well. There is an increase in the tensile strength by 19.9% and the strain is lower by 3%. There is a gain in tensile modulus by 25.97%.

Table 11. CFRP tensile test results

Material	**Maximum Force at Break (kN)**	**Maximum Stress (MPa)**	**Maximum Strain (%)**	**Tensile Modulus (GPa) (At ε_2=0.02% and ε_1=0.25%)**
Pure Epoxy	7116.20	284.65	1.90	13.59
1 wt.% GTP 475	8534.70	341.39	1.84	17.12

3.2.2. Bending Tests

3-point bending tests were performed on CFRP specimens doped with 1 wt.% of GTP 475. The bending stresses and flexural modulus were calculated from equations (4) and (5). The force versus deflection produced in the specimen is plotted below in Figure 34. The results of the tests are provided in Table 12 and Appendix 2.

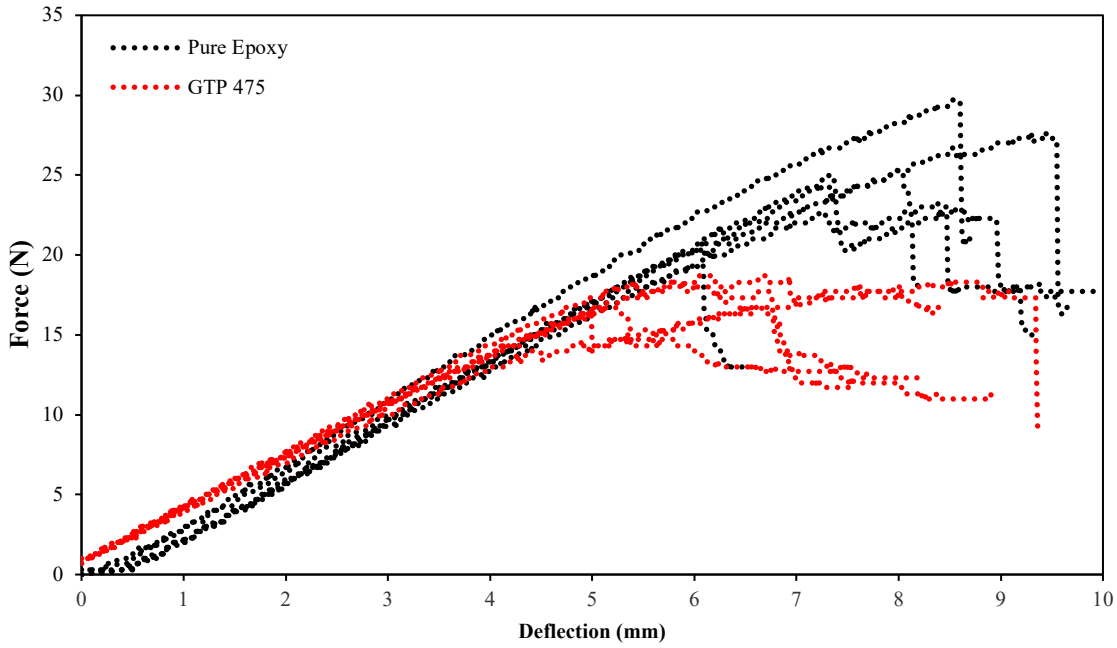

Fig. 34. Bending force vs deflection Plot

Table 12. Bending test results

Material	Maximum Bending Force (N)	Maximum Stress (MPa)	Deflection at Maximum Stress (mm)	Flexural Modulus (GPa)
Pure Epoxy	25.30	204.34	8.04	22.62
GTP 475	18.30	147.81	8.82	22.43

It is observed that the addition of GTP 475 has no significant impact on the flexural modulus of the specimen. The GTP 475 doped samples show higher deflection due to the inversely proportional relation between flexural modulus and deflection produced. The testing of flexural strength is similar to tensile testing as the specimens undergo tensile and compressive forces, however the difference between both is that in tensile testing the stress occurs throughout the area of the specimen while in bending tests, the stresses are concentrated in a certain area. The presence of voids and poor bonding of matrix and fibres significantly reduces the bending strength with a considerable small specimen size and thickness as there is a higher possibility of defects to be present in the tested area.

3.2.3. Impact Tests

Fibre reinforced epoxy specimens doped with 1 wt.% of GTP 475 were investigated under impact. For the test, the contact force (kN) and contact time (ms) were measured at every instant. The complete results of the test performed are given in Appendix 3. The force – time measurement from the impact test is plotted in Figure 35.

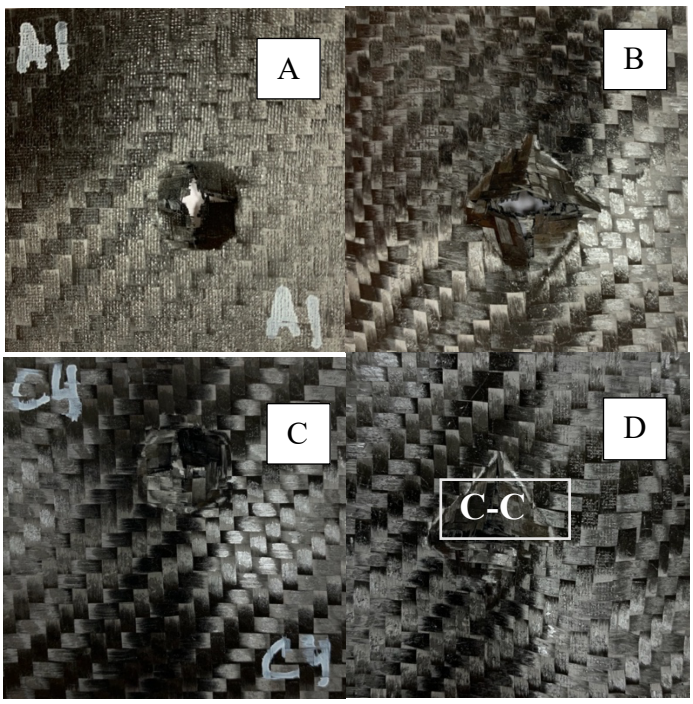

Fig. 35. Punctured impact test specimens (with top and bottom views) *A, B - pure epoxy*; *C, D - 1 wt.% GTP 475*.

Scanning electron microscopy (SEM) was performed on the impact specimens (cross section C-C) to assess the damage and various failure modes caused by the impact event. The images are discussed in detail in later sections *(Section 3.3)*.

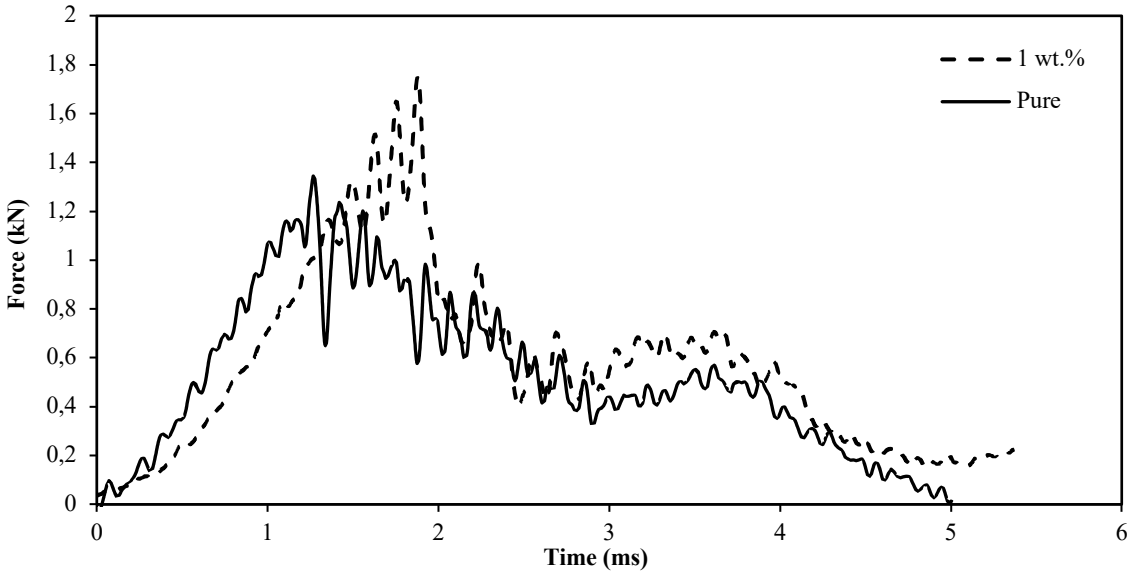

Fig. 36. Force-time graph for CFRP/GTP 475 specimens

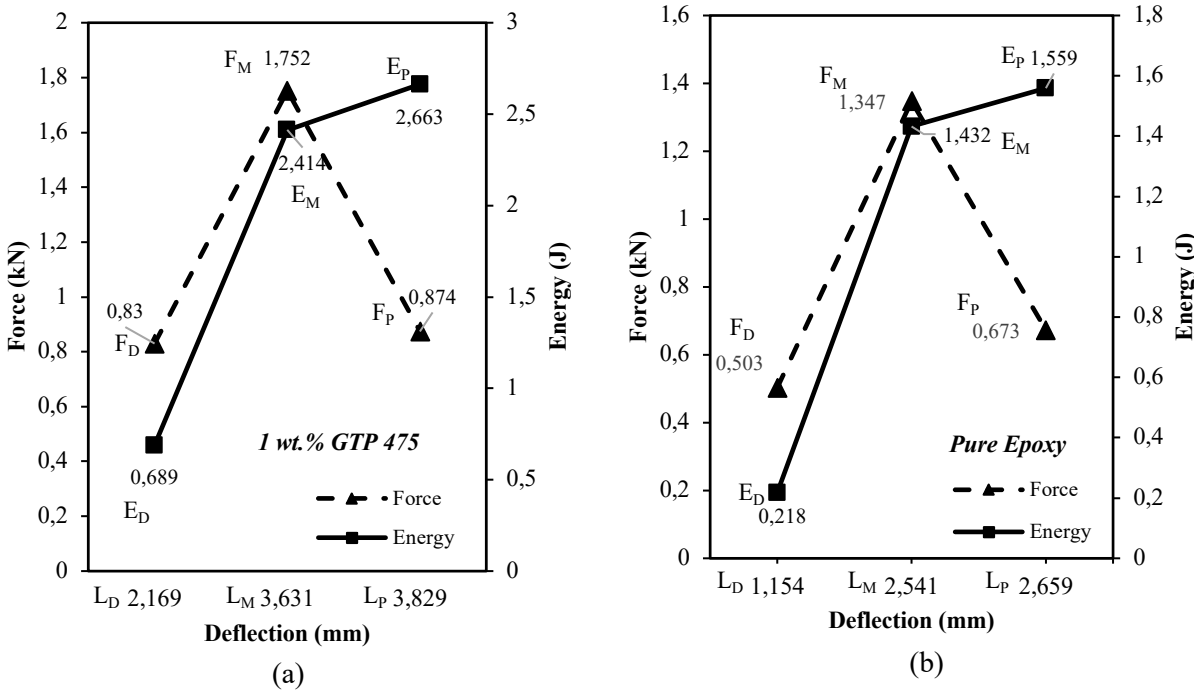

Fig. 37. Force-deflection-energy plots (a) – GTP 475 (b) – pure epoxy *F – force; L – deflection; E – energy; M – maximum; P – puncture; D – damage.*

These plots show that the force required to puncture the specimens of 1 wt. % is 1.75 kN, compared to 1.35 kN for pure epoxy showing higher force is required to puncture the specimen. The deflection at puncture for 1 wt.% GTP is 3.83 mm and higher absorption of energy is shown in Figure 36. The energies plotted above are at the point of damage, maximum force and point of puncture. The absorbed energy against the displacement is plotted below (Fig. 37).

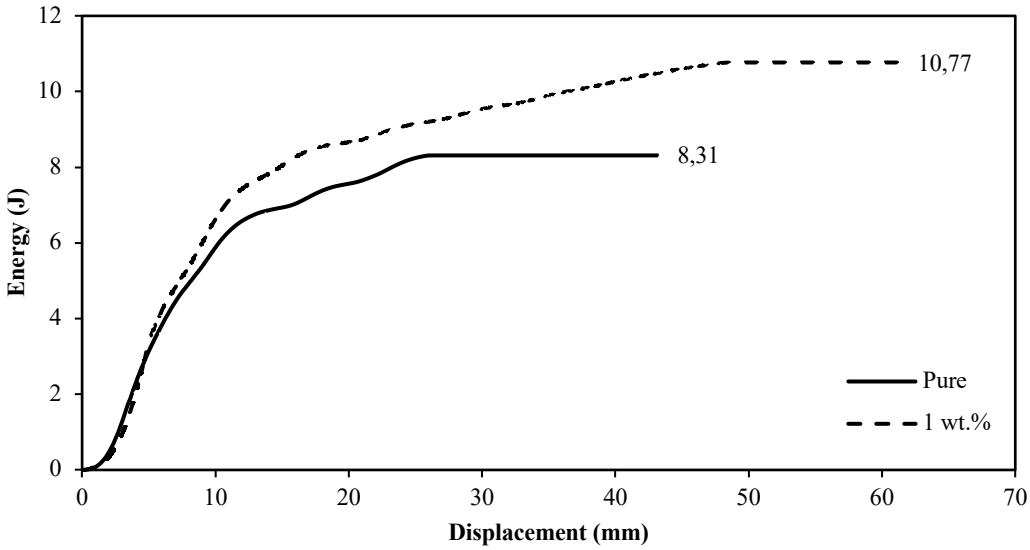

Fig. 38. Absorbed energy vs time plot

Figure 37 shows that energy absorbed by the additive specimens is 29.64% more than pure epoxy. Of the total impact energy of 20 J calculated by equation (7), the specimens absorbed 53.85% of the

energy. The SEM images discuss in detail the mode of failure and damage caused to the fibres and matrix.

3.3. SEM Analysis

Scanning electron microscopy (SEM) was performed on two sets of samples, tensile CFRP specimens doped with 3 wt.% of GTP 463 and impact CFRP specimens doped with 1% of GTP 475. Different failure modes have been captured, such as fibre rupture, fibre debonding, delamination, fibre pull-out.

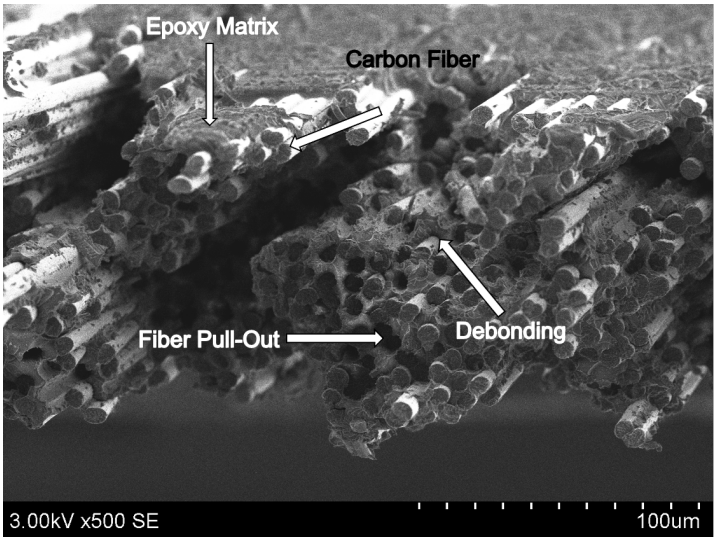

Fig. 39. SEM on CFRP/ GTP 463

Figure 39 displays the effects of tensile force acting on the fibres. There is fibre pull out and rupture at many places as shown above. The matrix has good adhesive properties and bonds with the fibre well. The fiber has been wetted out thoroughly and that matrix cracking is not visible. Micro-bubbles are not visible in the SEM pictures.

In Figure 40 it is observed that due to impact different modes of failure have occurred. Both inter and intralaminar delamination is observed (Fig. 40-B) and cusping due to shear acting between the fiber and matrix is detected (Fig 40-C). The matrix doped with GTP 475 shows good bonding between the fiber and matrix and elastic behavior in the matrix is observed (Fig. 40-A)

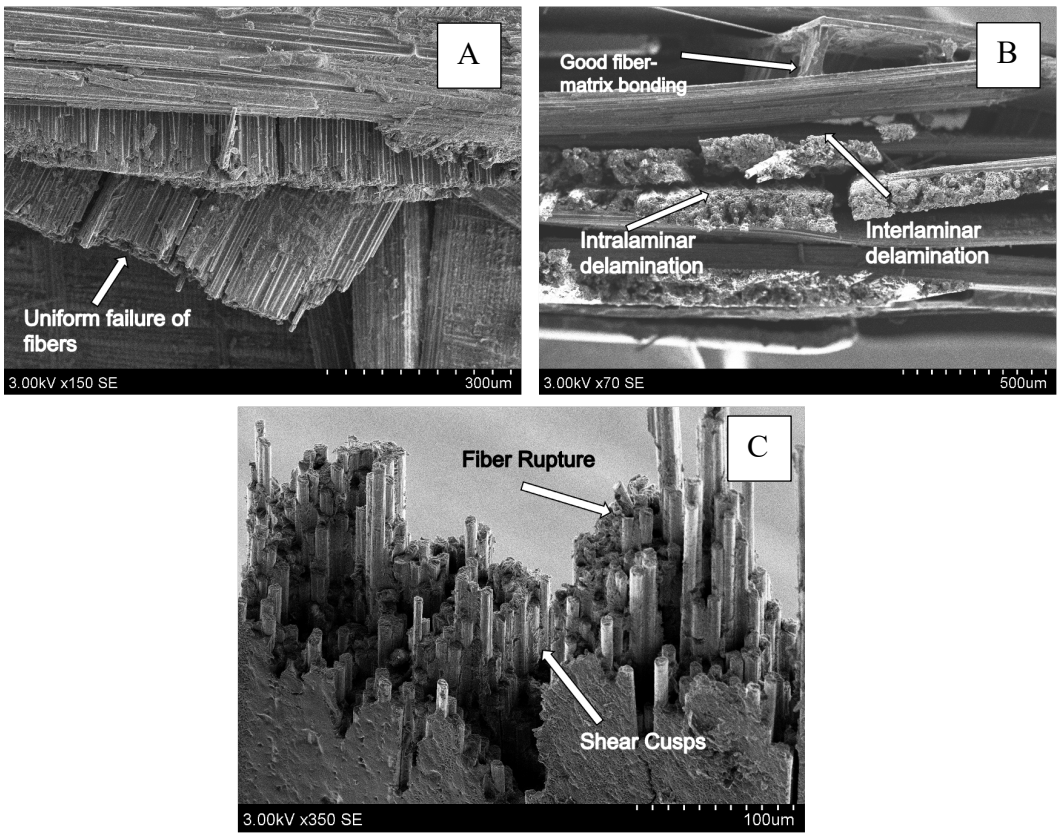

Fig. 40. SEM on CFRP/GTP 475

3.4. Comparative Analysis of Materials used in the Automotive Industry

From the above investigation, it is clearly noted that while the star-like additives do not make much of an improvement in the tensile and bending strengths of carbon fibre reinforced polymer composites, they have excellent energy absorbing qualities. Traditional materials buckle under impact while composites have various levels of failure such as matrix cracking, fibre rupture or debonding and delamination. These properties of composites can be altered to achieve a superior composite with higher strength to weight ratio.

For the evaluation of reliability of materials used as components in automotive, the concept of specific energy absorption (SEA) is critical. It is the amount of energy absorbed per unit mass of the material; therefore, it focuses on weight reduction. Focusing on the crumple zones present in automotive, it is crucial for the material to produce as much deformation and hence it is said that vehicles are made to crumple in the event of a collision. Like discussed before, the properties of the matrix define the composites' energy absorption capabilities. In this section, the various traditional materials versus composites and their SEA are discussed.

The equation to calculate specific energy absorption (SEA) is as follows:

$$SEA = \frac{Energy\ absorbed\ (J)}{Mass\ of\ the\ impact\ specimen\ (g)} \tag{7}$$

Ideally, SEA is calculated through crushing test on tubular specimens. A flat plate specimen will absorb 12% less energy than a tubular specimen since the width of the specimen does not contribute majorly to its energy absorption capability [51]. To calculate the SEA of the star doped specimens,

the weight damaged area is calculated approximately from the percentage of the specimen that has been damaged. Assuming that approximately 20% of the total area of the specimen is damaged,

Total mass of the specimen before impact = 1.45g

Therefore, the mass of the damaged area ~ 0.3g

Calculating SEA from equation 7 and plotting them alongside other materials being used in the undustry, we get Figure 41.

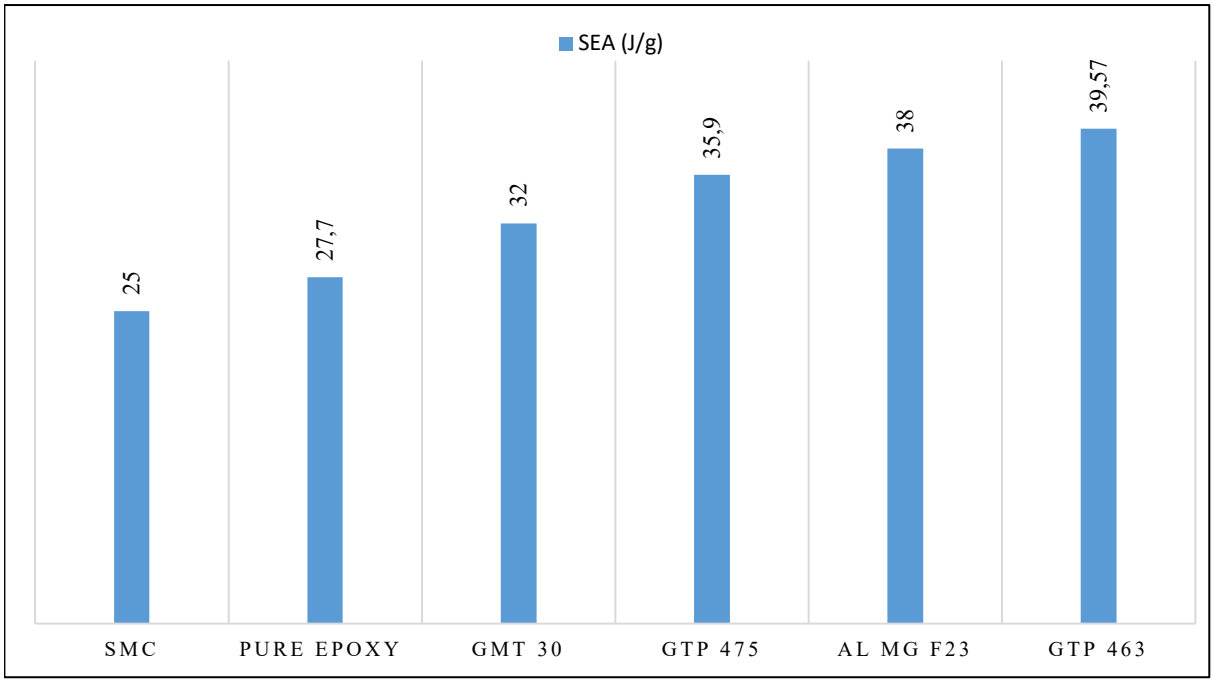

Fig. 41. SEA for different materials

This method of calculation of SEA is based on assumptions and more technical tests will need to be performed to measure exact absorption energy. Dynamic crushing tests will show exactly how energy can these stars absorb. However, the graph above depicts the potential of these stars and scope of development in the automotive industry.

Conclusions

1. The optimization of the matrix microstructure was carried out by performing tensile test on epoxy/additive specimens. The addition of 3 wt.% of GTP 463 in the epoxy matrix showed an improvement of tensile strength by 93.99% while an addition of 1 wt.% GTP 475 by 122%. These weight fractions were then reinforced with carbon fiber to test the improvement of its mechanical properties.
2. Experimental testing was performed on CFRP specimens to investigate mechanical properties. Tensile tests showed no improvement on addition of GTP 463 but an increase in the tensile modulus by 25.97% on addition of 1 wt.% of GTP 475. Flexural modulus of the composites increased with doping of GTP 463 by 16.27% and no improvement was observed on doping with GTP 475.
3. Low-velocity impact analysis was performed to examine the energy absorption capabilities of the CFRP doped with the additives. Both additives, GTP 463 and 475 performed well under impact. 3 wt.% of GTP 463 absorbed 37.5% of total impact energy while GTP 475 absorbed 53.85% of the energy.
4. A brief comparative analysis was performed with other materials used in automotive industry. Future potential is observed to develop these additives for excellent automotive component crashworthiness.

List of References

[1] "D Murali Manohar - Polymer Engineering PEB3213 - Polymer Composites Engineering 1," no. 1, pp. 1–22.

[2] N. Resources Canada, "Learn the facts: Weight affects fuel consumption What is the issue? What do I need to know?"

[3] K. Friedrich and A. A. Almajid, "Manufacturing aspects of advanced polymer composites for automotive applications," *Applied Composite Materials*, vol. 20, no. 2, pp. 107–128, Apr. 2013, doi: 10.1007/s10443-012-9258-7.

[4] L. Sanjay Mazumdar, "Driving Fuel Efficiency in the Automotive Industry Using Composites," p. 28, 2015.

[5] M. Applications and M. Fibers, *High-Performance and Specialty Fibers*. 2016. doi: 10.1007/978-4-431-55203-1.

[6] "Safety technology in Car: Crumple Zone." https://autoportal.com/articles/safety-technology-in-car-crumple-zone-2807.html (accessed May 03, 2021).

[7] G. Zhu, G. Sun, H. Yu, S. Li, and Q. Li, "Energy absorption of metal, composite and metal/composite hybrid structures under oblique crushing loading," *International Journal of Mechanical Sciences*, vol. 135, no. November, pp. 458–483, 2018, doi: 10.1016/j.ijmecsci.2017.11.017.

[8] J. Wang, C. Shi, N. Yang, H. Sun, Y. Liu, and B. Song, "Strength, stiffness, and panel peeling strength of carbon fiber-reinforced composite sandwich structures with aluminum honeycomb cores for vehicle body," *Composite Structures*, vol. 184, pp. 1189–1196, Jan. 2018, doi: 10.1016/j.compstruct.2017.10.038.

[9] Y. Hu, M. Yang, J. Zhang, C. Song, and T. Hong, "Effect of stacking sequence on the torsional stiffness of the composite drive shaft," *Advanced Composite Materials*, vol. 26, no. 6, pp. 537–552, Nov. 2017, doi: 10.1080/09243046.2016.1207126.

[10] G. Kelly, "Joining of Carbon Fibre Reinforced Plastics for Automotive Applications."

[11] H. Fukuda and T. W. Chou, "A probabilistic theory of the strength of short-fibre composites with variable fibre length and orientation," *Journal of Materials Science*, vol. 17, no. 4, pp. 1003–1011, Apr. 1982, doi: 10.1007/BF00543519.

[12] T. Ishikawa *et al.*, "Overview of automotive structural composites technology developments in Japan," *Composites Science and Technology*, vol. 155. Elsevier Ltd, pp. 221–246, Feb. 08, 2018. doi: 10.1016/j.compscitech.2017.09.015.

[13] F. Rezaei, R. Yunus, N. A. Ibrahim, and E. S. Mahdi, "Development of Short-Carbon-Fiber-Reinforced Polypropylene Composite for Car Bonnet," *Polymer-Plastics Technology and Engineering*, vol. 47, no. 4, pp. 351–357, Mar. 2008, doi: 10.1080/03602550801897323.

[14] P. Xiao, X. feng Lu, Y. Liu, and L. He, "Effect of in situ grown carbon nanotubes on the structure and mechanical properties of unidirectional carbon/carbon composites," *Materials Science and Engineering A*, vol. 528, no. 7–8, pp. 3056–3061, Mar. 2011, doi: 10.1016/j.msea.2010.11.067.

[15] H. Rong, K. H. Dahmen, H. Garmestani, M. Yu, and K. I. Jacob, "Comparison of chemical vapor deposition and chemical grafting for improving the mechanical properties of carbon fiber/epoxy composites with multi-wall carbon nanotubes," *Journal of Materials Science*, vol. 48, no. 14, pp. 4834–4842, Jul. 2013, doi: 10.1007/s10853-012-7119-2.

[16] N. Tsubokawa, "Preparation and properties of polymer-grafted carbon nanotubes and nanofibers," *Polymer Journal*, vol. 37, no. 9. Nature Publishing Group, pp. 637–655, Sep. 08, 2005. doi: 10.1295/polymj.37.637.

[17] R. He, Q. Chang, X. Huang, and J. bo, "Improved mechanical properties of carbon fiber reinforced PTFE composites by growing graphene oxide on carbon fiber surface," *Composite Interfaces*, vol. 25, no. 11, pp. 995–1004, Nov. 2018, doi: 10.1080/09276440.2018.1451677.

[18] M. Hossain *et al.*, "Enhanced mechanical properties of carbon fiber/epoxy composites by incorporating XD-grade carbon nanotube," *Journal of Composite Materials*, vol. 49, no. 18, pp. 2251–2263, Aug. 2015, doi: 10.1177/0021998314545186.
[19] X. Zhao, S. Qi, J. Liu, X. Han, and F. Zhang, "Preparation and mechanical performances of carbon fiber reinforced epoxy composites by MXene nanosheets coating," *Journal of Materials Science: Materials in Electronics*, vol. 30, no. 11, pp. 10516–10523, Jun. 2019, doi: 10.1007/s10854-019-01395-w.
[20] S. Aldajah and Y. Haik, "Transverse strength enhancement of carbon fiber reinforced polymer composites by means of magnetically aligned carbon nanotubes," *Materials and Design*, vol. 34, pp. 379–383, Feb. 2012, doi: 10.1016/j.matdes.2011.07.013.
[21] J. Leng *et al.*, "Analysis of Low-Velocity Impact Resistance of Carbon Fiber Reinforced Polymer Composites Based on the Content of Incorporated Graphite Fluoride," *Materials*, vol. 13, no. 1, p. 187, Jan. 2020, doi: 10.3390/ma13010187.
[22] Y. Zhou, F. Pervin, S. Jeelani, and P. K. Mallick, "Improvement in mechanical properties of carbon fabric–epoxy composite using carbon nanofibers," *Journal of Materials Processing Technology*, vol. 198, no. 1–3, pp. 445–453, Mar. 2008, doi: 10.1016/j.jmatprotec.2007.07.028.
[23] "POSS® (Polyhedral Oligomeric Silsesquioxane) Molecules." https://www.reade.com/products/poss-polyhedral-oligomeric-silsesquioxane-molecules (accessed Jun. 20, 2020).
[24] F. Zhao and Y. Huang, "Improved interfacial properties of carbon fiber/epoxy composites through grafting polyhedral oligomeric silsesquioxane on carbon fiber surface," *Materials Letters*, vol. 64, no. 24, pp. 2742–2744, Dec. 2010, doi: 10.1016/j.matlet.2010.08.074.
[25] F. Zhao and Y. Huang, "Grafting of polyhedral oligomeric silsesquioxanes on a carbon fiber surface: Novel coupling agents for fiber/polymer matrix composites," *Journal of Materials Chemistry*, vol. 21, no. 11, pp. 3695–3703, Mar. 2011, doi: 10.1039/c0jm03128c.
[26] L. Ma, Y. Zhu, M. Wang, X. Yang, G. Song, and Y. Huang, "Enhancing interfacial strength of epoxy resin composites via evolving hyperbranched amino-terminated POSS on carbon fiber surface," *Composites Science and Technology*, vol. 170, pp. 148–156, Jan. 2019, doi: 10.1016/j.compscitech.2018.12.001.
[27] X. Zhang, Y. Huang, T. Wang, and L. Hu, "Effects of silsesquioxane coating structure on mechanical interfacial properties of carbon fibre/polyarylacetylene composites," *Journal of Materials Science*, vol. 42, no. 13, pp. 5264–5271, Jul. 2007, doi: 10.1007/s10853-006-0349-4.
[28] F. Zhao, Y. Huang, L. Liu, Y. Bai, and L. Xu, "Formation of a carbon fiber/polyhedral oligomeric silsesquioxane/carbon nanotube hybrid reinforcement and its effect on the interfacial properties of carbon fiber/epoxy composites," *Carbon*, vol. 49, no. 8, pp. 2624–2632, Jul. 2011, doi: 10.1016/j.carbon.2011.02.026.
[29] H. Zhang *et al.*, "An experimental and analytical study of micro-laser line thermography on micro-sized flaws in stitched carbon fiber reinforced polymer composites," *Composites Science and Technology*, vol. 126, pp. 17–26, Apr. 2016, doi: 10.1016/j.compscitech.2016.02.007.
[30] T. Li, D. P. Almond, and D. A. S. Rees, "Crack imaging by scanning laser-line thermography and laser-spot thermography," *Measurement Science and Technology*, vol. 22, no. 3, 2011, doi: 10.1088/0957-0233/22/3/035701.
[31] A. Stamopoulos, K. Tserpes, P. Prucha, and D. Vavrik, "Evaluation of porosity effects on the mechanical properties of carbon fiber-reinforced plastic unidirectional laminates by X-ray computed tomography and mechanical testing," *Journal of Composite Materials*, vol. 50, no. 15, pp. 2087–2098, Jun. 2016, doi: 10.1177/0021998315602049.
[32] D. Saenz-Castillo, M. I. Martín, S. Calvo, F. Rodriguez-Lence, and A. Güemes, "Effect of processing parameters and void content on mechanical properties and NDI of thermoplastic

composites," *Composites Part A: Applied Science and Manufacturing*, vol. 121, pp. 308–320, Jun. 2019, doi: 10.1016/j.compositesa.2019.03.035.
[33] Y. Li, W. Zhang, Z. W. Yang, J. Y. Zhang, and S. J. Tao, "Low-velocity impact damage characterization of carbon fiber reinforced polymer (CFRP) using infrared thermography," *Infrared Physics and Technology*, vol. 76, pp. 91–102, May 2016, doi: 10.1016/j.infrared.2016.01.019.
[34] H. Fernandes, C. Ibarra-Castanedo, H. Zhang, and X. Maldague, "Thermographic Non-destructive Evaluation of Carbon Fiber-Reinforced Polymer Plates After Tensile Testing," *Journal of Nondestructive Evaluation*, vol. 34, no. 4, pp. 1–10, Nov. 2015, doi: 10.1007/s10921-015-0303-y.
[35] R. Gutkin, C. J. Green, S. Vangrattanachai, S. T. Pinho, P. Robinson, and P. T. Curtis, "On acoustic emission for failure investigation in CFRP: Pattern recognition and peak frequency analyses," *Mechanical Systems and Signal Processing*, vol. 25, no. 4, pp. 1393–1407, May 2011, doi: 10.1016/j.ymssp.2010.11.014.
[36] J. M. Park, D. S. Kim, J. R. Lee, and T. W. Kim, "Nondestructive damage sensitivity and reinforcing effect of carbon nanotube/epoxy composites using electro-micromechanical technique," *Materials Science and Engineering C*, vol. 23, no. 6–8, pp. 971–975, Dec. 2003, doi: 10.1016/j.msec.2003.09.131.
[37] J. Wen, Z. Xia, and F. Choy, "Damage detection of carbon fiber reinforced polymer composites via electrical resistance measurement," *Composites Part B: Engineering*, vol. 42, no. 1, pp. 77–86, Jan. 2011, doi: 10.1016/j.compositesb.2010.08.005.
[38] S. Wang and D. D. L. Chung, "Mechanical damage in carbon fiber polymer-matrix composite, studied by electrical resistance measurement," in *Composite Interfaces*, 2002, vol. 9, no. 1, pp. 51–60. doi: 10.1163/156855402753642890.
[39] S. Wang, D. Wang, D. D. L. Chung, and J. H. Chung, "Method of sensing impact damage in carbon fiber polymer-matrix composite by electrical resistance measurement," *Journal of Materials Science*, vol. 41, no. 8, pp. 2281–2289, Apr. 2006, doi: 10.1007/s10853-006-7172-9.
[40] "(No Title)." http://www.ezentrumbilder.de/rg/pdf/td_en_190225NA.pdf (accessed May 03, 2021).
[41] J. F. Johnson and R. S. Porter, "Gel permeation chromatography," *Progress in Polymer Science*, vol. 2, no. C, pp. 811–820, 1970, doi: 10.1016/S0079-6700(70)80005-3.
[42] "2.2: Molecular Weight Determination - Chemistry LibreTexts." https://chem.libretexts.org/Bookshelves/Analytical_Chemistry/Book%3A_Physical_Methods_in_Chemistry_and_Nano_Science_(Barron)/02%3A_Physical_and_Thermal_Analysis/2.02%3A_Molecular_Weight_Determination (accessed May 03, 2021).
[43] "ISO - ISO 527-2:2012 - Plastics — Determination of tensile properties — Part 2: Test conditions for moulding and extrusion plastics." https://www.iso.org/standard/56046.html (accessed May 04, 2021).
[44] F. Taheri-Behrooz, M. M. Shokrieh, and H. R. Abdolvand, "Designing and manufacturing of a drop weight impact test machine," *Engineering Solid Mechanics*, vol. 1, no. 2, pp. 69–76, 2013, doi: 10.5267/j.esm.2013.08.001.
[45] F. Kiehas, A. Kalteis, M. Jerabek, and Z. Major, "Experimental investigation of the failure behaviour of polypropylene compounds for instrumented puncture tests," *16th Youth Symposium on Experimental Solid Mechanics, YSESM 2018*, pp. 66–71, 2018, doi: 10.14311/APP.2018.18.0066.
[46] "12.3 Stress, Strain, and Elastic Modulus - University Physics Volume 1 | OpenStax." https://openstax.org/books/university-physics-volume-1/pages/12-3-stress-strain-and-elastic-modulus (accessed May 05, 2021).
[47] "(No Title)." https://core.ac.uk/download/pdf/11013041.pdf (accessed May 10, 2021).

Appendices

Appendix 1. Tensile Results

CFRP/Pure Epoxy				
Sample No.	**Maximum Force at Break (kN)**	**Maximum Stress (MPa)**	**Maximum Strain (%)**	**Tensile Modulus (GPa)** (At $\boldsymbol{\varepsilon_2}$=0.02% and $\boldsymbol{\varepsilon_1}$=0.25%)
1	9332.30	373.29	2.34	12.89
2	10062.10	402.48	2.42	12.75
3	7116.20	284.65	1.90	13.59
4	8829.00	353.16	2.06	14.61
5	8987.9	359.52	2.48	11.87
6	9223.4	368.94	1.98	15.30

CFRP/3 wt.% GTP 463				
Sample No.	**Maximum Force at Break (kN)**	**Maximum Stress (MPa)**	**Maximum Strain (%)**	**Tensile Modulus (GPa)** (At $\boldsymbol{\varepsilon_2}$=0.02% and $\boldsymbol{\varepsilon_1}$=0.25%)
1	11851.50	474.06	3.14	13.05
2	7884.30	315.37	1.98	11.92
3	9926.70	397.07	1.92	13.97
4	10100.40	404.01	2.28	14.71

CFRP/1 wt.% GTP 475				
Sample No.	**Maximum Force at Break (kN)**	**Maximum Stress (MPa)**	**Maximum Strain (%)**	**Tensile Modulus (GPa)** (At $\boldsymbol{\varepsilon_2}$=0.02% and $\boldsymbol{\varepsilon_1}$=0.25%)
1	10062.10	402.48	2.42	13.15
2	9912.00	396.48	2.3	12.84
3	8534.70	341.39	1.84	17.12
4	9461.70	378.47	2.32	15.41
5	9606.00	384.24	2.16	15.59

Appendix 2. Bending Test Results

CFRP/Pure Epoxy			
Sample No.	**Maximum Force at Break (N)**	**Maximum Bending Stress (MPa)**	**Deflection at Maximum Force (mm)**
1	25.30	204.34	8.04
2	19.30	155.88	6.09
3	29.70	239.88	8.60
4	22.30	180.11	8.96
5	18.00	145.38	9.19
6	27.70	223.73	9.30

CFRP/3 wt.% GTP 463			
Sample No.	**Maximum Force at Break (N)**	**Maximum Bending Stress (MPa)**	**Deflection at Maximum Force (mm)**
1	19.00	153.46	5.15
2	21.00	169.62	5.44
3	20.30	163.96	7.45
4	20.30	163.96	5.98
5	19.00	153.46	6.98
6	21.00	169.17	6.07

CFRP/1 wt.% GTP 475			
Sample No.	**Maximum Force at Break (N)**	**Maximum Bending Stress (MPa)**	**Deflection at Maximum Force (mm)**
1	18.70	151.04	6.73
2	18.30	147.81	5.89
3	16.70	134.88	5.25
4	16.70	134.88	6.65
5	18.30	147.81	8.82

Appendix 3. Impact Test Results

Pure Epoxy

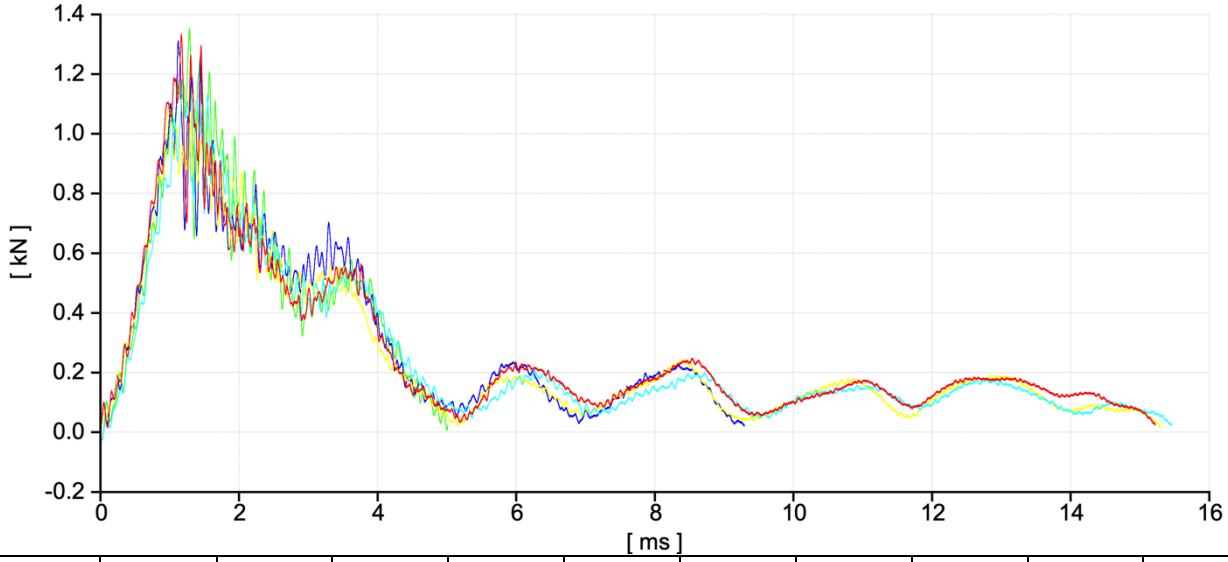

Sample	T (mm)	I_d (mm)	F_d (kN)	E_d (J)	I_m (mm)	F_m (kN)	E_m (J)	I_p (mm)	F_p (kN)	E_p (J)
1	1.000	1.294	0.620	0.342	2.311	1.326	1.308	3.686	0.662	2.551
2	1.000	1.154	0.503	0.218	2.541	1.347	1.432	2.659	0.673	1.559
3	1.000	1.054	0.486	0.213	2.222	1.305	1.155	3.554	0.652	2.348
4	1.000	1.095	0.493	0.230	1.968	1.083	0.878	4.308	0.540	2.849
5	1.000	1.168	0.430	0.190	2.345	1.126	1.076	4.547	0.563	2.910

3 wt.% GTP 463

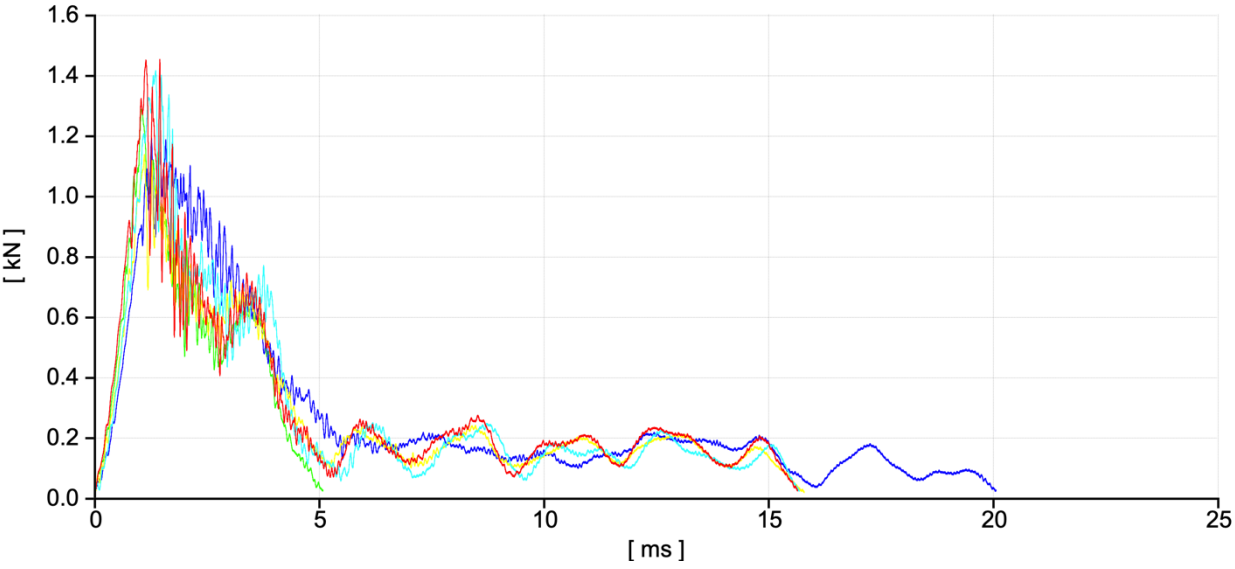

Sample	T (mm)	I_d (mm)	F_d (kN)	E_d (J)	I_m (mm)	F_m (kN)	E_m (J)	I_p (mm)	F_p (kN)	E_p (J)
1	1.000	1.497	0.915	0.614	2.802	1.448	2.108	2.883	0.723	2.197
2	1.000	1.207	0.591	0.341	2.024	1.347283	1.092	3.587	0.642	2.597
3	1.000	1.931	0.871	0.708	2.477	1.189	1.240	6.317	0.594	4.682

4	1.000	1.202	0.535	0.295	2.163	1.133	1.094	4.729	0.566	3.111
5	1.000	1.487	0.715	0.442	2.647	1.411	1.712	3.862	0.705	2.960

1 wt.% GTP 475

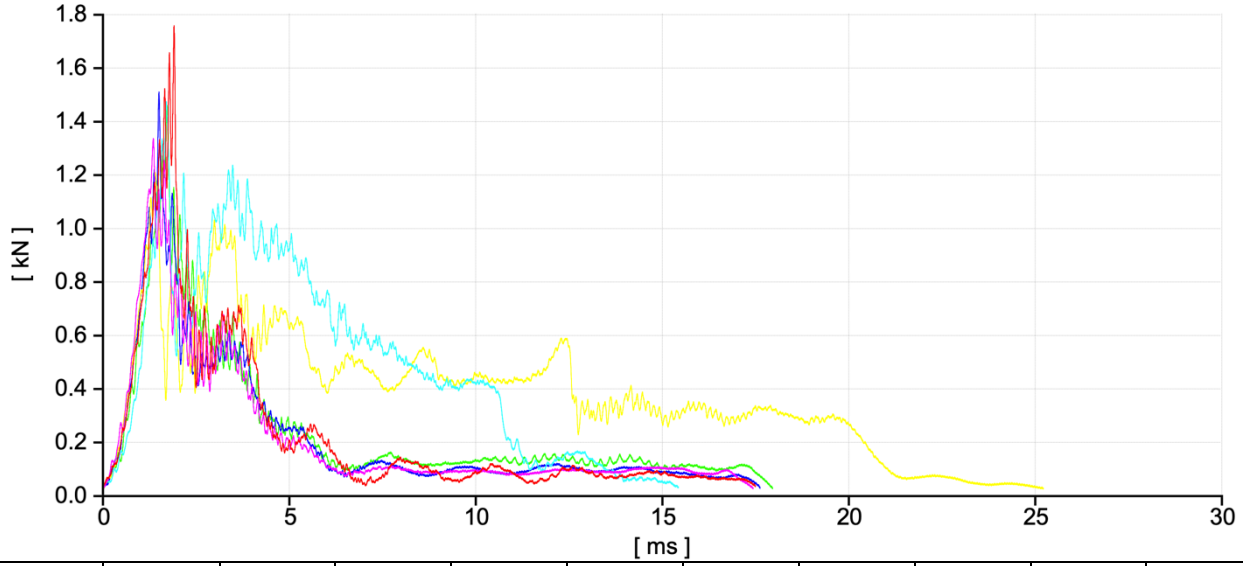

Sample	**T (mm)**	**I_d (mm)**	**F_d (kN)**	**E_d (J)**	**I_m (mm)**	**F_m (kN)**	**E_m (J)**	**I_p (mm)**	**F_p (kN)**	**E_p (J)**
1	1.000	2.169	0.830	0.689	3.631	1.752	2.414	3.829	0.874	2.663
2	1.000	1.798	0.582	0.380	3.313	1.453	1.774	4.301	0.726	2.711
3	1.000	2.406	1.073	0.048	2.890	1.504	1.491	3.845	0.750	2.445
4	1.000	2.006	0.764	0.609	2.698	1.203	1.275	3.110	0.601	1.648
5	1.000	2.422	0.853	0.686	3.288	1.468	1.628	3.648	0.734	2.009
6	1.000	2.393	1.141	1.049	2.603	1.330	1.301	3.510	0.665	2.230